Designs for Computer Experiments that Minimize the Weighted Integrated Mean Square Prediction Error

Erin R. Leatherman
Department of Statistics, West Virginia University

Angela M. Dean
Department of Statistics, The Ohio State University

Thomas J. Santner
Department of Statistics, The Ohio State University

February 10, 2014

Abstract

Computer experiments based on deterministic simulators can sometimes be used to replace or supplement physical experiments. This paper studies the construction and predictive performance of designs obtained using integrated mean square prediction error (IMSPE) and Weighted IMSPE (W-IMSPE) criteria. While IMSPE-based criteria use predictors exactly tuned to the process generating the data, a simulation study shows that empirical best linear unbiased predictors (EBLUPs) with parameters estimated from the data of IMSPE-based designs improve upon the predictive accuracy of EBLUPs formed from space-filling designs. Best IMSPE- and W-IMSPE-optimal designs are recommended for practice.

Keywords: Experimental design; Gaussian process interpolator; IMSPE; Emulator; Kriging; Simulator

1 Introduction

A *deterministic computer simulator* is the implementation in computer code of a mathematical model that describes the relationship between input and output variables in a physical system. As mathematical descriptions have become more sophisticated, the use of deterministic simulators as experimental vehicles has become more widespread in applications such as engineering design (for example, the design and wear of tool coatings in Nekkanty (2009) and, more generally, Forrester, Sobester, and Keane (2008)), biomechanics (Ong, Santner, and Bartel 2008), the physical sciences (Higdon, Kennedy, Cavendish, Cafeo, and Ryne 2004), the life sciences (Upton, Guilak, Laursen, and Setton 2006; Fogelson, Kuharsky, and Yu 2003), public policy (Lempert, Schlensinger, Bankes, and Andronova 2000), and population biology (Hajagos 2005).

As in any experiment, a *computer experiment* is performed by varying the inputs to the simulator and observing the effects on the simulator output. Computer experiments are sometimes used instead of traditional physical experiments when the number of experimental factors is too numerous to study via a physical experiment, when a physical experiment is financially prohibitive, or when conducting a physical experiment is unethical.

In some cases the desired computer simulator is expensive to evaluate and can require days or even months to run, see for example Hayeck (2009) or Ong et al. (2008). This paper assumes that a fast-running and reasonably accurate emulator of the simulator output can be obtained based on a Gaussian Process (GP) model. It assumes that the GP model parameters are unknown and must be estimated using the data from a "well-chosen" set of simulator inputs (training data). Output from this emulator can then be used to make predictions of simulator output (e.g. Sacks, Schiller, and Welch 1989a; Sacks, Welch, Mitchell, and Wynn 1989b; Currin, Mitchell, Morris, and Ylvisaker 1991; Santner, Williams, and Notz 2003).

Broadly, two classes of designs for running computer experiments have been considered in the literature: space-filling designs and process-based designs. Some comparisons of designs for computer experiments can be found in Bates, Buck, Riccomagno, and Wynn (1996), Koehler and Owen (1996), Bursztyn and Steinberg (2006), and Johnson, Jones, Fowler, and Montgomery (2008).

Space-filling designs include uniform designs (Wang and Fang 1981; Fang, Lin, Winker,

and Zhang 2000), maximin and minimax designs (Johnson, Moore, and Ylvisaker 1990), minimum average reciprocal distance designs (Audze and Eglais 1977; Bates, Sienz, and Toropov 2003; Liefvendahl and Stocki 2006), and lattice designs (Niederreiter 1992; Bates et al. 1996). Often a space-filling design is selected by one of the above criteria from the class of Latin hypercube designs (Morris and Mitchell 1995), which were originally proposed for integration (McKay, Beckman, and Conover 1979) and which ensure the design has a uniform projection in each individual input dimension.

In contrast, process-based design criteria make use of an emulator of the (future) simulator output. Process-based design criteria include minimum Integrated Mean Squared Prediction Error (IMSPE) (Sacks et al. 1989a,b), maximum entropy (Shewry and Wynn 1987; Currin et al. 1991; Mitchell and Scott 1987), and maximum expected improvement (Bernardo, Buck, Liu, Nazaret, Sacks, and Welch 1992; Jones, Schonlau, and Welch 1998). Optimal process-based designs are more problematic to construct than space-filling designs because they require complete specification of the interpolating process, e.g., the mean and covariance/correlation of a GP emulator. However it is often the case that the specific values of such parameters are not known. In some cases, subject-matter knowledge about the parameters may be available. In other cases, the parameters must be estimated only from training data collected during the initial runs of the simulator. This paper assumes that sufficient information about the interpolating model parameters is available such that the minimum Weighted Integrated Mean Squared Prediction Error (W-IMSPE) design criterion can be applied to determine the training data used to make simulator predictions at untested input sites.

The organization of the paper follows. Section 2 presents the GP model of simulator output and the corresponding best linear unbiased predictor (BLUP) of the output at untested inputs. Section 3 uses this model and BLUP to specify IMSPE and W-IMSPE design criteria. Section 4 discusses computational methods used to construct the optimal designs considered in this paper. Section 5 presents the correlation weight functions (priors, for Bayesians) used to construct W-IMSPE-optimal designs, and examples of these designs. A simulation study in Section 6 demonstrates that empirical versions of the BLUP based on W-IMSPE- and IMSPE-optimal designs provide more accurate predictions of simulator output than do empirical BLUPs (EBLUPs) based on traditionally-used space-filling designs; this section

also makes design recommendations. Section 7 discusses limitations and extensions of the results.

2 Statistical Model and Prediction

Let $y(\boldsymbol{x})$ denote the real-valued output of a computer simulator for $\boldsymbol{x} \in \mathcal{X}$, a $d \times 1$ input vector, where $\mathcal{X}$ is a d-dimensional, rectangular input space that is scaled to $[0,1]^d$. As in Sacks et al. (1989a,b) and Currin et al. (1991), the deterministic computer simulator outputs are modeled as realizations of the GP

$$Y(\boldsymbol{x}) = \sum_{i=1}^{p} f_i(\boldsymbol{x})\beta_i + Z(\boldsymbol{x}) = \boldsymbol{f}^T(\boldsymbol{x})\boldsymbol{\beta} + Z(\boldsymbol{x}), \tag{1}$$

where $\boldsymbol{f}^T(\cdot) = (f_1(\cdot), f_2(\cdot), \ldots, f_p(\cdot))$ are known regression functions, $\boldsymbol{\beta} = (\beta_1, \beta_2, \ldots, \beta_p)^T$ is a vector of unknown regression coefficients, and deviations from the regression are modeled by $Z(\cdot)$, a zero-mean, stationary GP over $\mathcal{X}$ with variance σ_Z^2 , and product Gaussian correlation function

$$\text{Cor}\left(Y(\boldsymbol{x}_u), Y(\boldsymbol{x}_v)\right) = R(\boldsymbol{x}_u - \boldsymbol{x}_v \mid \boldsymbol{\rho}) = \prod_{j=1}^{d} \rho_j^{4(x_{uj} - x_{vj})^2}, \tag{2}$$

where $\rho_j \in [0,1]$ for $1 \le j \le d$ and x_{uj} is the j^{th} element of input $\boldsymbol{x}_u$, $1 \le u \le n$ (Higdon et al. (2004)). Here $\boldsymbol{\rho} = (\rho_1, \rho_2, \ldots, \rho_d)^T$, and ρ_j is the correlation between the outputs at two inputs that differ only in the j^{th} dimension by half their domain. The equivalent parameterization $\gamma_j = -4\ln(\rho_j)$, $1 \le j \le d$, of (2) is often used so that $\rho_j^{4(\cdot)^2} = e^{-\gamma_j(\cdot)^2}$ and $\gamma_j \ge 0$. However, the methodology in this paper does not rely on the use of the Gaussian correlation function (2), so alternative correlation functions, such as those in Section 2.3.3 of Santner et al. (2003), could be used instead.

Suppose that n simulator outputs $y(\boldsymbol{x}_1), y(\boldsymbol{x}_2), \ldots, y(\boldsymbol{x}_n)$ are observed at n training inputs represented by the rows of the $(n \times d)$ design matrix $\boldsymbol{X} = [\boldsymbol{x}_1, \boldsymbol{x}_2, \ldots, \boldsymbol{x}_n]^T$. Informally, the set of d-dimensional input points $\{\boldsymbol{x}_i \in \mathcal{X}, 1 \le i \le n\}$ will be referred to as "the $n \times d$ design $\boldsymbol{X}$" and the set of all such designs will be denoted by $\mathcal{D}_{n,d}$.

Sacks et al. (1989a) show that when the correlation parameters $\boldsymbol{\rho}$ are known but $\boldsymbol{\beta}$ is un-

known, the best linear unbiased predictor of $y(\boldsymbol{x}_0)$, based on $\boldsymbol{y}^n = (y(\boldsymbol{x}_1), y(\boldsymbol{x}_2), \ldots, y(\boldsymbol{x}_n))^T$, is

$$\widehat{y}(\boldsymbol{x}_0) = \boldsymbol{f}_0^T \widehat{\boldsymbol{\beta}} + \boldsymbol{r}_0^T \boldsymbol{R}^{-1}(\boldsymbol{y}^n - \boldsymbol{F}\widehat{\boldsymbol{\beta}}), \tag{3}$$

where $\boldsymbol{f}_0 = \boldsymbol{f}(\boldsymbol{x}_0)$ is the $p \times 1$ vector of known regressors at $\boldsymbol{x}_0$; $\boldsymbol{F}$ is the $n \times p$ matrix of known regressors having $(i,j)^{\text{th}}$ element $f_j(\boldsymbol{x}_i)$ for $1 \leq i \leq n, 1 \leq j \leq p$; $\boldsymbol{r}_0$ is the $n \times 1$ vector $(R(\boldsymbol{x}_0 - \boldsymbol{x}_1), \ldots, R(\boldsymbol{x}_0 - \boldsymbol{x}_n))^T$ and $\boldsymbol{R}$ is the $n \times n$ matrix $(R(\boldsymbol{x}_i - \boldsymbol{x}_j))$ whose elements are defined by the correlation function (2); and $\widehat{\boldsymbol{\beta}} = (\boldsymbol{F}^T \boldsymbol{R}^{-1} \boldsymbol{F})^{-1} \boldsymbol{F}^T \boldsymbol{R}^{-1} \boldsymbol{y}^n$ is the generalized least squares estimator of $\boldsymbol{\beta}$.

Prediction based on the GP model (1) is popular for many reasons. First, the predictor is semi-parametric; the long-run trend mean structure is specified by a regression while local deviations from the trend are described by a stationary GP. Second, when GP parameters are known, the conditional distribution (and conditional mean) used to predict new output values based on current runs and to quantify uncertainty about the estimated output are simple to obtain. Third, the (empirical) BLUPs based on this model interpolate the data at the training data inputs, which is desirable when the computer simulator produces deterministic output.

The predictor in (3) will be used to construct IMSPE- and W-IMSPE-optimal designs in Section 3. Later, Section 6 will compare the predictive ability of (3) with restricted maximum likelihood (REML) plug-in estimates for $\boldsymbol{\rho}$, based on training data obtained from various designs.

3 Design Criteria for Prediction

When considering designs for a computer experiment, the simulator is often treated as a "black-box" function, meaning that the relationship between the inputs and outputs is completely unknown. In such cases, space-filling designs have been suggested for computer experiments in order to explore the entire input space, see Bates et al. (1996). The simulation study in Section 6 includes two types of space-filling designs: the maximin Latin hypercube design (Johnson et al. 1990) and the minimum average reciprocal distance Latin hypercube design (Audze and Eglais 1977; Bates et al. 2003; Liefvendahl and Stocki 2006). These designs will be compared with process-based designs obtained under the minimum

IMSPE and the minimum W-IMSPE criteria defined below.

IMSPE and W-IMSPE criteria focus on good prediction. The predictor $\widehat{y}(\boldsymbol{x}_0)$ in (3) depends on $\boldsymbol{X}$ and on the model parameters (through $\boldsymbol{F}, \boldsymbol{r}_0$, and $\boldsymbol{R}$). For fixed design $\boldsymbol{X}$, $\boldsymbol{\rho}$, and σ_Z^2, one measure of prediction ability at $\boldsymbol{x}_0$ is the mean squared prediction error (MSPE) of $\widehat{y}(\boldsymbol{x}_0)$ which is

$$\text{MSPE}\left(\boldsymbol{x}_0, \boldsymbol{X} \mid \sigma_Z^2, \boldsymbol{\rho}\right) = \sigma_Z^2 \left(1 - \begin{bmatrix} \boldsymbol{f}_0^T & \boldsymbol{r}_0^T \end{bmatrix} \begin{bmatrix} \boldsymbol{0}_{p\times p} & \boldsymbol{F}_{n\times p}^T \\ \boldsymbol{F}_{n\times p} & \boldsymbol{R}_{n\times n} \end{bmatrix}^{-1} \begin{bmatrix} \boldsymbol{f}_0 \\ \boldsymbol{r}_0 \end{bmatrix}\right), \tag{4}$$

where $\boldsymbol{0}_{p\times p}$ is a $p \times p$ matrix of zeros and the implicit expectation in (4) is taken over the joint distribution of $(Y(\boldsymbol{x}_0), \boldsymbol{Y}^n)$ with $\boldsymbol{Y}^n = (Y(\boldsymbol{x}_1), Y(\boldsymbol{x}_2), \ldots, Y(\boldsymbol{x}_n))^T$.

An IMSPE-optimal design in $\mathcal{D}_{n,d}$ minimizes the MSPE (4) averaged over the input space $\mathcal{X}$. Formally, the IMSPE is

$$\begin{aligned} \text{IMSPE}\left(\boldsymbol{X} \mid \sigma_Z^2, \boldsymbol{\rho}\right) &= \int_{\mathcal{X}} \text{MSPE}\left(\boldsymbol{w}, \boldsymbol{X} \mid \sigma_Z^2, \boldsymbol{\rho}\right) \mathrm{d}\boldsymbol{w} \\ &= \sigma_Z^2 \left(1 - \text{trace}\left(\begin{bmatrix} \boldsymbol{0} & \boldsymbol{F}^T \\ \boldsymbol{F} & \boldsymbol{R} \end{bmatrix}^{-1} \int_{\mathcal{X}} \begin{pmatrix} \boldsymbol{f}_{\boldsymbol{w}} \boldsymbol{f}_{\boldsymbol{w}}^T & \boldsymbol{f}_{\boldsymbol{w}} \boldsymbol{r}_{\boldsymbol{w}}^T \\ \boldsymbol{r}_{\boldsymbol{w}} \boldsymbol{f}_{\boldsymbol{w}}^T & \boldsymbol{r}_{\boldsymbol{w}} \boldsymbol{r}_{\boldsymbol{w}}^T \end{pmatrix} \mathrm{d}\boldsymbol{w}\right)\right), \end{aligned} \tag{5}$$

when $\boldsymbol{\rho}$ and σ_Z^2 are known (see Sacks et al. (1989a,b) for calculation details). Formula (5) can be expressed in terms of the univariate standard Normal distribution for the Gaussian correlation function (2). A design $\boldsymbol{X}_I$ that minimizes

$$\text{IMSPE}^\star\left(\boldsymbol{X} \mid \boldsymbol{\rho}\right) \equiv \text{IMSPE}\left(\boldsymbol{X} \mid \sigma_Z^2 = 1, \boldsymbol{\rho}\right) \tag{6}$$

also minimizes $\text{IMSPE}\left(\cdot \mid \sigma_Z^2, \boldsymbol{\rho}\right)$ for all $\sigma_Z^2 > 0$. Therefore the IMSPE optimal design is defined in terms of IMSPE*.

This paper considers the case where the correlation parameters $\boldsymbol{\rho}$ that need to be specified to calculate IMSPE* are not known, but information about either the range or more detailed subject matter knowledge of the possible values of $\boldsymbol{\rho}$ is available. In this case, an average of the IMSPE* values with weights $\pi\left(\boldsymbol{\rho}\right)$ is an appropriate criterion. From a Bayesian perspective, the weight $\pi\left(\boldsymbol{\rho}\right)$ is a prior distribuion. This results in the *Weighted Integrated*

Mean Square Prediction Error (W-IMSPE) design objective function

$$W(\boldsymbol{X}) = \int_{[0,1]^d} \text{IMSPE}^{\star}(\boldsymbol{X} \mid \boldsymbol{\rho})\, \pi(\boldsymbol{\rho})\, \mathrm{d}\boldsymbol{\rho}. \tag{7}$$

A design $\boldsymbol{X}_W$ that minimizes (7) is a W-IMSPE-optimal design.

Using training data determined by a minimum W-IMSPE design is desirable for use in a computer experiment because it ensures that the predictor $\widehat{y}(\cdot)$ is close to the computer simulator output $y(\cdot)$, on average, over the entire input space $\mathcal{X}$, as well as over the correlation parameter spaces weighed according to $\pi(\boldsymbol{\rho})$. It will be shown in Section 6 that these designs perform well over a range of example surfaces. In the next section, computational issues arising in the calculation of the W-IMSPE objective function are discussed.

4 Computational Methods for W-IMSPE-optimal Design Construction

The sections that follow describe how the numerical evaluation of the W-IMSPE objective function was performed and the optimization methods used in this paper to find the W-IMSPE-optimal designs studied in Section 6. To avoid the numerical complication of calculating W-IMSPE when design points $\{\boldsymbol{x}_i\}$ are "too close" together, which leads to a numerically non-invertible correlation matrix $\boldsymbol{R}$, an ϵ-*ball* of radius 10^{-3} is placed around each design point.

4.1 Numerical Evaluation of the W-IMSPE Objective Function

Because closed-form evaluation of W-IMSPE is not available, numerical integration was used to calculate (7). Many methods of numerical integration from the the numerical analysis literature have been used in statistics; two recent surveys of these methods are Kincaid and Cheney (2002) and Givens and Hoeting (2012). This paper used Sobol´ sequences to perform Quasi-Monte Carlo integration of (7) (Morokoff and Caflisch (1995) and Niederreiter (1992));

thus the W-IMSPE formula is approximated by

$$W\left(\boldsymbol{X}\right) \approx \sum_{j=1}^{2^k} \text{IMSPE}^{\star}\left(\boldsymbol{X} \mid \boldsymbol{\rho}_j\right) \pi\left(\boldsymbol{\rho}_j\right), \tag{8}$$

where $\boldsymbol{\rho}_j$ is the j^{th} point of the 2^k-point Sobol´ sequence in d dimensions. The d correlation parameters are taken to be mutually independent, so $\pi(\rho_1, \ldots, \rho_d) = \prod_{i=1}^{d} \pi_i(\rho_i)$ where $\pi_i(\cdot)$ is the probability density of ρ_i.

Two techniques were implemented to enhance the computational accuracy of (8): a rescaling and shifting of the $\{\boldsymbol{\rho}_j\}_{j=1}^{2^k}$ points, and selecting the minimally accurate k. The first technique is based on the observation that, for fixed k and the selected $\pi(\cdot)$, many terms in (8) can have very small $\pi(\boldsymbol{\rho}_j)$. One can improve the accuracy of (8) by increasing the number of $\boldsymbol{\rho}_j$ having significant $\pi\left(\boldsymbol{\rho}_j\right)$ contributions to (8). This can be accomplished by transforming the range of integration of each $\boldsymbol{\rho}_j$ from $[0,1]^d$ to $\prod_{i=1}^{d}[a_i, b_i]$, where $0 < a_i < b_i < 1$ are selected so that all component pdfs $\pi_i(\rho_i)$, $1 \le i \le d$, of $\pi(\boldsymbol{\rho})$ satisfy

$$\pi_i(\rho_i) \ge 10^{-10} \text{ for } \rho_i \in [a_i, b_i], \tag{9}$$

ignoring the constant of proportionality that this induces on the right side of (8). For the $d = 2, 3, 5$ used in this paper, all univariate prior ranges $[a_i, b_i]$ were selected to satisfy (9). When d is "large", say $d = 20$, the bounds (9) can still result in very small $\pi(\boldsymbol{\rho})$ for many of the terms in the Sobol´ sequence. In this case, a value larger than 10^{-10} could, after appropriate accuracy studies, be used in (9).

The second method of increasing the accuracy of (8) while ensuring computationally feasibility is to select the minimal k so that (8) computed with 2^k terms provides a 'good' estimate of W-IMSPE (7). The length of the Sobol´ sequence needed to estimate (7) well is tied to d, the dimension of the integral. As d in (7) increases, longer Sobol´ sequences are needed for (8) to approximate (7) accurately. For the examples in this paper, k was chosen to be 11 for $d = 2$, 16 for $d = 3$, and 17 for $d = 5$. This selection was determined by calculating W-IMSPE (8) for several designs using an array of k values, and selecting the smallest k for which W-IMSPE converged numerically. Unfortunately, because the computation time needed to evaluate (8) doubles as k increases to $k+1$, the use of $k = 16$ and 17 to find the W-

IMSPE-optimal designs for $d = 3$ and 5, respectively, became computationally prohibitive. Instead, an adaptive number of draws was used in the optimization. This method will be described in Section 4.2

4.2 Design Optimization

This paper used a combination of Particle Swarm Optimization (PSO) and gradient-based quasi-Newton (QN) optimization to find the $n \times d$ design $\boldsymbol{X}$ that minimizes W-IMSPE (8) for the input space, $\mathcal{X} = [0,1]^d$. To find a W-IMSPE-optimal design of size (n, d) for a specific $\pi(\boldsymbol{\rho})$, a modified particle swarm optimization (PSO) was used to identify a design that served as the starting point for a QN search for the best design; a detailed description of this heuristic approach is presented in Leatherman, Dean, and Santner (2014).

The basic PSO algorithm for this application is described first, then modifications that are used herein are given. The PSO algorithm of Kennedy and Eberhart (1995) was implemented using N_{des} $n \times d$ starting designs $\boldsymbol{X}_i^1$, $1 \leq i \leq N_{\text{des}}$, called "particles". Each design $\boldsymbol{X}_i^1$ was reshaped (column-wise) into an $nd \times 1$ vector $\boldsymbol{z}_i^1 = vec\,(\boldsymbol{X}_i^1)$. To ensure the initial designs were well spread in nd-space, the initial set of N_{des} designs were selected so that $\left[\boldsymbol{z}_1^1, \boldsymbol{z}_2^1, \ldots, \boldsymbol{z}_{N_{\text{des}}}^1\right]^\top$ formed an approximate *maximin LHD*.

Each particle was updated a given number, N_{its}, of times. The update step from $\boldsymbol{z}_i^t$ to $\boldsymbol{z}_i^{t+1}$, $1 \leq i \leq N_{\text{des}}$ and $1 \leq t \leq N_{\text{its}}$, is a randomly weighted step towards the current global-best position,

$$\boldsymbol{g}^t \equiv \underset{s \in \{1,2,\ldots,t\},\, i \in \{1,2,\ldots,N_{\text{des}}\}}{\operatorname{argmin}} W\left(\boldsymbol{X}_i^s\right).$$

and the current design-best position

$$\boldsymbol{p}_i^t \equiv \underset{s \in \{1,2,\ldots,t\}}{\operatorname{argmin}} W\left(\boldsymbol{X}_i^s\right).$$

The update is

$$\boldsymbol{z}_i^{t+1} = \boldsymbol{z}_i^t + \boldsymbol{v}_i^{t+1}, \tag{10}$$

where "velocity" $\boldsymbol{v}_i^{t+1} = \gamma \boldsymbol{v}_i^t + \alpha \boldsymbol{\epsilon_1}_i^t \circ (\boldsymbol{g}^t - \boldsymbol{z}_i^t) + \beta \boldsymbol{\epsilon_2}_i^t \circ (\boldsymbol{p}_i^t - \boldsymbol{z}_i^t)$ and $\circ$ denotes the element-wise product of comparable vectors. Following the recommendations of Kennedy and Eberhart (1995) and Yang (2010), designs in this paper were constructed using step weights $\alpha =$

$\beta = 2$, inertia parameter $\gamma = 0.5$, initial velocity $\boldsymbol{v}_i^1 = \mathbf{0}_{nd}$, and independent random vectors $\boldsymbol{\epsilon_1}_i^t$ and $\boldsymbol{\epsilon_2}_i^t$ whose elements are independent Uniform[0,1], for $1 \leq i \leq N_{\text{des}}$ and $1 \leq t \leq N_{\text{its}}$. Additionally, the random velocity vectors $\boldsymbol{v}_i^t$ were bounded component-wise by $[-0.25 \times \mathbf{1}_{nd}, 0.25 \times \mathbf{1}_{nd}]$. For this paper, components of the velocity vectors $\boldsymbol{v}_i^t$ falling outside of the bounds were relocated to the boundary of the velocity domain in each dimension for which this occurred. Additionally, any element of $\boldsymbol{z}_i^t$ moved outside of $[0,1]^{nd}$ was relocated to the boundary of $[0,1]^{nd}$ in each dimension in which the violation occurred. Finally, the PSO algorithm was run with $N_{\text{its}} = 2 \times N_{\text{des}}$ iterations and $N_{\text{des}} = 4 \times n \times d$ initial designs.

To provide computational feasibility, the PSO algorithm was modified using an adaptive number of Sobol´ draws. The idea is that initially a smaller k can be used because $W(\boldsymbol{X})$ differences are likely to be larger while bigger k values must be used when making the final $W(\boldsymbol{X})$ comparisons because these values are likely to be more nearly equal. Specifically, for each starting design $\boldsymbol{X}_i^1$, $1 \leq i \leq N_{\text{des}}$, approximately the first 90% of the N_{its} iterations were performed with a 'cheaply' estimated $W(\boldsymbol{X})$ by calculating (8) with 2^{11} Sobol´ draws. The remaining 10% of the iterations used the more accurate k for the d of interest.

A second modification of the PSO algorithm was made to enhance the ability of the algorithm to escape from local minima. A randomly selected set of 5% of the N_{des} designs that were evolved after 90% of the PSO iterations were replaced by a space-filling set of alternative designs. Then the remaining 10% of the PSO iterations were conducted starting with this modified set of designs (and using the more accurate k). Recalling that each design is a $nd \times 1$ vector, the alternative designs where taken to be the rows of an (approximate) maximin Latin hypercube containing $0.05 \times N_{des}$ rows and nd columns.

After the remaining 10% of the iterations were performed using the larger number of Sobol´ draws, the best design constructed by PSO was taken as the starting design for a single run of a QN algorithm (as implemented in the MATLAB code `fmincon.m`) to produce the final design. The QN algorithm used the larger, d-dependent, k value to calculate (8).

5 W-IMSPE-optimal Designs

This section lists the specific correlation values, $\boldsymbol{\rho}_0$, used to construct IMSPE-optimal designs and the specific correlation weight functions, $\pi(\boldsymbol{\rho})$, used to construct W-IMSPE-optimal designs for the simulation study in Section 6. All IMSPE- and W-IMSPE-optimal designs in this paper were constructed using a constant mean $\boldsymbol{f}^T(\boldsymbol{x})\boldsymbol{\beta} = \beta_0$ for the GP (1). This section also shows an example of a W-IMSPE-optimal design that was constructed using the computational methods described in Section 4 and compares it to a maximin design for the same (n, d).

5.1 Selection of Correlation Weights

Four IMSPE-optimal designs were found corresponding to minimizing $\text{IMSPE}^\star(\boldsymbol{X}|\boldsymbol{\rho}_0)$ for four choices of $\boldsymbol{\rho}_0$ and four W-IMSPE-optimal designs were constructed corresponding to four non-degenerate $\pi(\boldsymbol{\rho})$. Note that IMSPE-optimal designs can also be considered W-IMSPE-optimal designs that are constructed with a degenerate prior. The $\boldsymbol{\rho}_0$ for three of the IMSPE-optimal designs contained a common correlation value in all dimensions: $\boldsymbol{\rho}_0 = 0.25 \times \mathbf{1}_d, 0.50 \times \mathbf{1}_d$, and $0.75 \times \mathbf{1}_d$. These point masses and their corresponding designs are denoted $\text{I}_{.25}$, $\text{I}_{.5}$, and $\text{I}_{.75}$ in Table 1. The fourth $\boldsymbol{\rho}_0$ varied correlation values across input dimensions; some correlations were set to reflect high activity ($\rho = 0.25$) and others to reflect low activity ($\rho = 0.75$). Specifically, for $d = 2$, $\boldsymbol{\rho}_0 = [0.75, 0.25]^T$; for $d = 3$, $\boldsymbol{\rho}_0 = [0.75, 0.25, 0.25]^T$; and for $d = 5$, $\boldsymbol{\rho}_0 = [0.75, 0.75, 0.25, 0.25, 0.25]^T$. This point mass and its corresponding IMSPE-optimal design are denoted I_M in Table 1.

The first non-degenerate $\pi(\boldsymbol{\rho})$ is the (non-informative) uniform weight on $[0.01, 0.99]^d$; that is, $\pi(\boldsymbol{\rho}) = \left(\frac{1}{0.99-0.01}\right)^d$ for $\boldsymbol{\rho} \in [0.01, 0.99]^d$. The uniform prior and its corresponding W-IMSPE-optimal design are denoted W^U in Table 1. The remaining three non-degenerate $\pi(\boldsymbol{\rho})$ were of the form $\prod_{i=1}^d \pi(\rho_i)$, with a common, marginal beta density for independent ρ_i, $1 \leq i \leq d$. The first two marginal densities, beta$(5, 13)$ and beta$(15, 43)$, were specified by selecting integer parameters that yielded a mode of 0.25 and standard deviations of 0.10 and 0.0570, respectively. The third marginal density, beta$(37.96, 37.96)$, has mode 0.50 and standard deviation 0.0570, which is the same standard deviation as the beta$(15, 43)$ weight function. These three weight functions and their corresponding W-IMSPE-optimal designs

are denoted $\mathrm{W}_{W}^{.25}$, $\mathrm{W}_{N}^{.25}$, and $\mathrm{W}_{N}^{.5}$ in Table 1, where the superscripts represent the mode of the distribution and the subscripts W and N represent "wide" and "narrow" distribution spread.

Table 1: Labels for the weight functions and correlation values used in the calculation of W-IMSPE-optimal and IMSPE-optimal designs. For $\mathrm{W}_{W}^{.25}$, $\mathrm{W}_{N}^{.25}$, and $\mathrm{W}_{N}^{.5}$ the support of the distribution is determined by (9).

Label	Correlation $\boldsymbol{\rho}_0$
$\mathrm{I}_{.25}$	$0.25 \times \mathbf{1}_d$
$\mathrm{I}_{.5}$	$0.50 \times \mathbf{1}_d$
$\mathrm{I}_{.75}$	$0.75 \times \mathbf{1}_d$
I_{M}	$(0.75, 0.25)^T$, $d = 2$ $(0.75, 0.25, 0.25)^T$, $d = 3$ $(0.75, 0.75, 0.25, 0.25, 0.25)^T$, $d = 5$

Label	Weight $\pi(\cdot)$ in $\prod_{i=1}^{d} \pi(\rho_i)$
$\mathrm{W}_{W}^{.25}$	$\pi(\rho) \propto \rho^4 (1-\rho)^{12}$
$\mathrm{W}_{N}^{.25}$	$\pi(\rho) \propto \rho^{14} (1-\rho)^{42}$
$\mathrm{W}_{N}^{.5}$	$\pi(\rho) \propto \rho^{36.96} (1-\rho)^{36.96}$
W^{U}	$\pi(\rho) = \left(\frac{1}{0.99-0.01}\right) \times \mathrm{I}_{(\rho \in [0.01, 0.99])}$

5.2 Example of a W-IMSPE Design

In total, thirty-two W-IMSPE- (IMSPE-)optimal designs were constructed corresponding to the four (n, d) combinations in $\{(10, 2), (15, 3), (30, 3), (16, 5)\}$ and the eight weight functions listed in Table 1.

While the full set of designs is presented in Appendix A of the Supplementary Material, one specific example is examined here. This design is an $n = 30$-run W-IMSPE-optimal design for the $\mathrm{W}_{W}^{.25}$ weight function over the input space $[0, 1]^3$ (the points of the design are listed in Table 22 in the Supplementary Material). The 1-d and 2-d projections of this design, presented in Figure 1, show that the projected points are somewhat clustered. However, when viewed in the full 3-d input space, the points of this design appear more space-filling; the minimum 3-d Euclidean interpoint distance is 0.2975. Additionally, none

Figure 1: Two-dimensional projections of a 30-run W-IMSPE-optimal design in $[0,1]^3$ constructed using the W_W^{25} weight function.

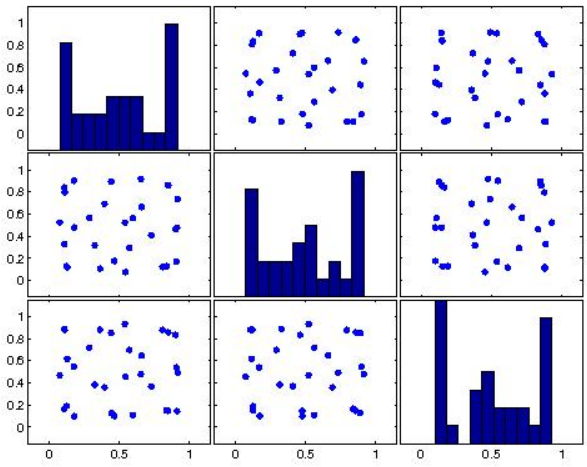

of the points in this design lie on a boundary of $[0,1]^3$; in fact, all points are located within $[0.06, 0.94]^3$.

For comparison, a 30-run maximin Euclidean interpoint distance design in $[0,1]^3$ was obtained from the website of Specht (2013). The 1-d and 2-d projections of this design are plotted in Figure 2. In both lower dimensions, the projections are more grid-like than for the W_W^{25}-optimal design. By construction, the minimum 3-d interpoint distance is larger for this design (0.4714) than for the W_W^{25}-optimal design (0.2975). Also, many of the maximin design points lie on a boundary of $[0,1]^3$.

6 Design Comparison

6.1 Prediction Accuracy

Because this paper assumes that prediction is of primary interest, the design objective function W-IMSPE is based on the MSPE building block (4) which describes an ideal circumstance in which simulator test surfaces are drawn from a GP with known parameters and prediction is performed using (3) which also assumes knowledge of the GP parameters.

Section 6 uses simulation to compare designs constructed for the utopian predictor of

Figure 2: Two-dimensional projections of a 30-run maximin Euclidean interpoint distance design in $[0,1]^3$ obtained from Specht (2013).

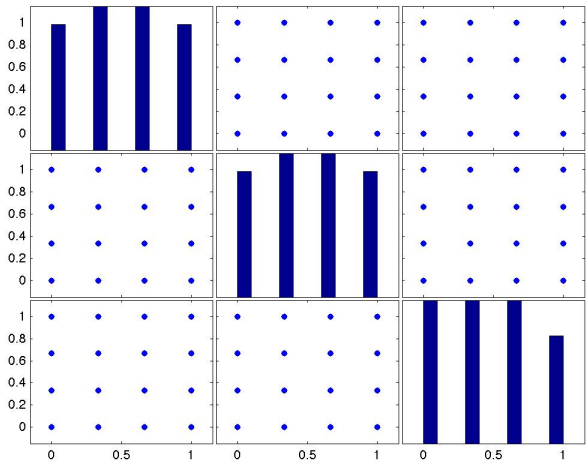

Section 2 by their predictive accuracy when using a widely-employed EBLUP with estimated parameters. The predictor used is the EBLUP

$$\widehat{y}^E(\boldsymbol{x}_0) = \widehat{\beta}_0 + \widehat{\boldsymbol{r}}_0^T \widehat{\boldsymbol{R}}^{-1} \left(\boldsymbol{y}^n - \mathbf{1}_n \widehat{\beta}_0 \right), \tag{11}$$

based on the constant-mean GP with unknown process variance σ_Z^2 and having Gaussian correlation function (2) with unknown correlations $\boldsymbol{\rho} = (\rho_1, \ldots, \rho_d)^T$. Here $\boldsymbol{y}^n$ is defined following (3), while $\widehat{\beta}_0 = \left(\mathbf{1}_n^T \widehat{\boldsymbol{R}}^{-1} \boldsymbol{y}^n \right) / \left(\mathbf{1}_n^T \widehat{\boldsymbol{R}}^{-1} \mathbf{1}_n \right)$, $\mathbf{1}_n$ is a column vector of n ones, and $\widehat{\boldsymbol{r}}_0$ and $\widehat{\boldsymbol{R}}$ are defined analogously to $\boldsymbol{r}_0$ and $\boldsymbol{R}$ but in terms of an estimated correlation function $\widehat{R}(\cdot \mid \widehat{\boldsymbol{\rho}})$ instead of the known correlation function $R(\cdot \mid \boldsymbol{\rho})$. In this paper $\widehat{\boldsymbol{\rho}}$ is the REML estimate of $\boldsymbol{\rho}$.

Using a given design, $\boldsymbol{X}$, training data is collected from a specified test-bed output function $y(\boldsymbol{x})$ (see Section 6.3). Then REML estimates of $\boldsymbol{\rho}$ are calculated (using the MATLAB Parametric Empirical Kriging (MPErK) (2013) software). The empirical mean square prediction error (EMSPE)

$$\text{EMSPE}(\boldsymbol{X}) = \frac{1}{6^d} \sum_{i=1}^{6^d} \left(\widehat{y}^E(\boldsymbol{x}_i) - y(\boldsymbol{x}_i) \right)^2 \tag{12}$$

over an equally-spaced grid of 6^d points in $[0,1]^d$ is used to quantify the predictive accuracy when using design $\boldsymbol{X}$.

6.2 Designs Studied

For each $(n,d) \in \{(10,2),(15,3),(30,3),(16,5)\}$, ten designs were compared using EMSPE. The designs are described below and, in brief, include space-filling, IMSPE-optimal and W-IMSPE-optimal designs. The two space-filling designs used were a maximin Latin hypercube design (MmLHD) under L2 distance (Johnson et al. 1990; Morris and Mitchell 1995) and a minimum average reciprocal distance Latin hypercube design (mARDLHD) (Audze and Eglais 1977; Liefvendahl and Stocki 2006). Both space-filling designs were obtained from the website of van Dam, den Hertog, Husslage, and Rennen (2013), and are listed in Appendix D of the Supplementary Material.

The four IMSPE-optimal designs $\mathrm{I}_{.25}, \mathrm{I}_{.5}, \mathrm{I}_{.75}$, and I_M in Table 1, were constructed by using the PSO plus QN optimization algorithm of Section 4.2 to minimize $\mathrm{IMSPE}^\star(\boldsymbol{X} \mid \boldsymbol{\rho})$ in (6) for the constant-mean GP model. Similarly the four W-IMSPE-optimal designs $\mathrm{W}_W^{.25}, \mathrm{W}_N^{.25}, \mathrm{W}_N^{.5}$, and W^U in Table 1 were calculated for the constant-mean GP model using the integration methods and the modified PSO plus QN algorithm described in Section 4.

6.3 The Test-Bed of $y(\cdot)$ Functions

A test-bed of non-linear surfaces was created using the method of Trosset (1999) to compare the predictive capability of the designs described in Section 6.2. In this application of Trosset (1999), each test surface is a Kriging interpolator of the form

$$y_{\text{test}}(\boldsymbol{w}) = \hat{\beta}_0 + \boldsymbol{r}(\boldsymbol{w})^T \boldsymbol{R}^{-1} \left(\boldsymbol{Y}^{500} - \mathbf{1}_{500} \hat{\beta}_0 \right), \ \boldsymbol{w} \in [0,1]^d . \tag{13}$$

based on 500 draws from a GP. Specifically, $\boldsymbol{Y}^{500}$ was a 500×1 vector drawn from a GP at an approximate maximin $500 \times d$ LHD in $[0,1]^d$, $\boldsymbol{L}$. The GP had mean 100, variance 10, and Gaussian correlation function (2), where $\boldsymbol{\rho} = [\rho_1, \rho_2, \ldots, \rho_d]^T$ was specified to be one of seven correlation settings described below. For numerical stability, a nugget of size 10^{-6} was added to the diagonal of the GP's covariance matrix, $\sigma^2 \boldsymbol{R}$. In $y_{\text{test}}(\boldsymbol{w})$, $\boldsymbol{r}(\boldsymbol{w})$ is the

500×1 vector of correlations ($R(\boldsymbol{x}_i, \boldsymbol{w})$) for $\boldsymbol{x}_i^T \in \boldsymbol{L}$, $\boldsymbol{R}$ is the 500×500 matrix of correlations ($R(\boldsymbol{x}_i, \boldsymbol{x}_j) + \delta_{i=j}(10^{-6})$) for $\boldsymbol{x}_i^T, \boldsymbol{x}_j^T \in \boldsymbol{L}$, and $\widehat{\beta}_0 = \left(\mathbf{1}_{500}^T \boldsymbol{R}^{-1} \boldsymbol{Y}^{500}\right) / \left(\mathbf{1}_{500}^T \boldsymbol{R}^{-1} \mathbf{1}_{500}\right)$.

To compare the designs described in Section 6.2, seven correlation families were used to generate a test-bed of response surfaces. For each correlation setting, 40 surfaces $y_{\text{test}}(\boldsymbol{w})$ were taken as representative computer simulators of that setting. The seven correlation families can be grouped into three categories:

1. *Deterministically Common Correlation:* Three test-beds $y_{\text{test}}(\cdot)$ correspond to $\rho_1 = \rho_2 = \ldots = \rho_d = \rho$ where $\rho \in \{0.25, 0.50, 0.75\}$. These families are denoted $\text{T}_{.25}^{DC}$, $\text{T}_{.5}^{DC}$, and $\text{T}_{.75}^{DC}$, respectively. Because the correlation parameters are of equal size for a given correlation family, each input dimension has the same opportunity to influence the output.

2. *Stochastically Common Correlation:* Three test beds $y_{\text{test}}(\cdot)$ correspond to independent and identically distributed $\rho_1, \rho_2, \ldots, \rho_d$ drawn from one of the following distributions: beta$(5, 13)$, beta$(11.34, 11.34)$, and beta$(13, 5)$. These families are denoted $\text{T}_{.25}^{SC}$, $\text{T}_{.5}^{SC}$, and $\text{T}_{.75}^{SC}$, respectively, where the subscript denotes the mode of the distribution. The values of the correlation parameters are not necessarily equal within a single vector draw; thus, the d inputs are allowed to have unequal influences on the output. Given one of the three parameter distributions, a separate $d \times 1$ vector of correlation parameters is drawn independently to create each of the 40 $y_{\text{test}}(\boldsymbol{w})$.

3. *Mixed Activity Correlation:* The final set of correlation parameters is selected so that some inputs have a strong effect on the output (high activity) while others do not affect the output substantially (low activity). Inputs having high activity correspond to ρ_H, which are drawn independently from a Uniform(0.1, 0.5) distribution for each high activity input, and inputs having low activity correspond to ρ_L, which are drawn independently from a Uniform(0.90, 0.99) distribution for each low activity input. This family is denoted T^M and includes $\boldsymbol{\rho} = [\rho_L, \rho_H]^T$ for $d = 2$, $\boldsymbol{\rho} = [\rho_L, \rho_H, \rho_H]^T$ for $d = 3$, and $\boldsymbol{\rho} = [\rho_L, \rho_L, \rho_H, \rho_H, \rho_H]^T$ for $d = 5$. A separate $d \times 1$ vector of correlation parameters is drawn independently to create each of the 40 $y_{\text{test}}(\boldsymbol{w})$.

For each correlation family, 40 correlation parameter vectors are selected. Each vector of correlation parameters is inserted in (2) and $\boldsymbol{Y}^{500}$ is drawn to construct a test surface (13).

A total of $280 = 7 \times 40$ surfaces was drawn for each input size $d = 2, 3, 5$; the same 280 surfaces were used to test both the 15×3 and 30×3 designs.

6.4 Results and Recommendations

After creating a test-bed of 280 $y_{\text{test}}(\boldsymbol{w})$ surfaces for each of the dimensions $d = 2, 3, 5$, training data were collected from the surfaces using each of the ten designs described in Section 6.2. For each set of training data, predictions $\widehat{y}^E(\cdot)$ were made at an equally-spaced input grid of 6^d points. Each grid of predictions was used to calculate EMSPE (12) for a particular design and test surface combination.

Figure 3: Boxplots of 40 EMSPE values for test-bed $\mathrm{T}_{.25}^{DC}$ and the $(n, d) = (30, 3)$ designs. The mean EMSPE for each design is plotted as a solid circle, and the smallest 75^{th} percentile among the 10 designs is denoted by a horizontal line.

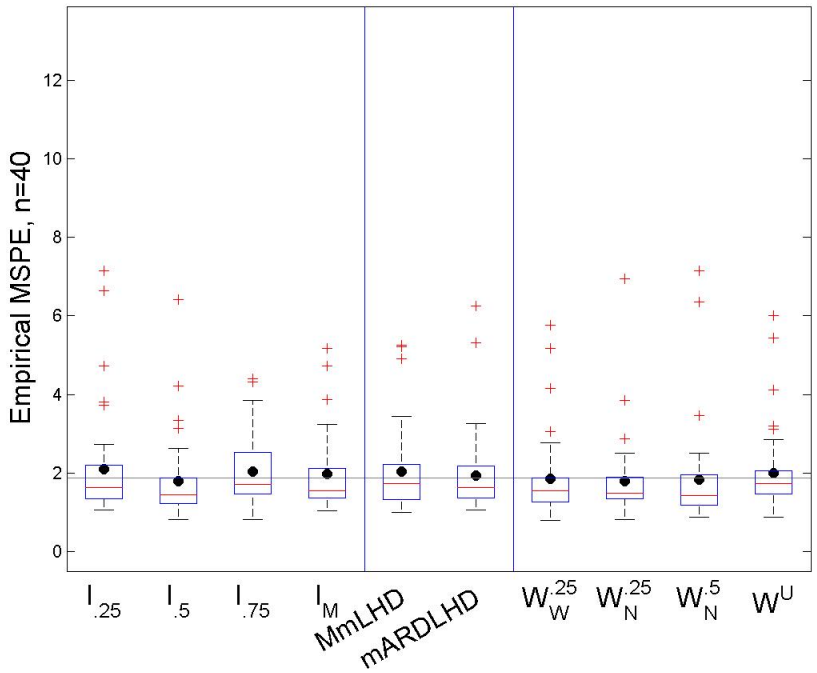

The 40 EMSPE values were collected for all test surface and design combinations. Figure 3 shows boxplots of EMSPE values for each 30×3 design studied using the test-bed $\mathrm{T}_{.25}^{DC}$. In this figure, the mean EMSPE for each design is plotted as a solid circle. The 75^{th} percentiles of the EMSPE values were calculated for each combination of design and test-bed correlation setting. For the 30×3 designs, these percentiles are summarized by design type

and correlation setting in Table 2. Corresponding tables for the other design sizes are found in Appendix B of the Supplementary Material.

Table 2: The 75$^{\text{th}}$ percentile of the 40 EMSPE values for the 10 designs and the 7 test-bed correlation settings studied when $(n, d) = (30, 3)$.

Design		$y_{\text{test}}(\cdot)$ Test-bed Correlation Setting						
		Deterministically Common			*Stochastically Common*			*Mixed Activity*
		$\text{T}_{.25}^{DC}$	$\text{T}_{.5}^{DC}$	$\text{T}_{.75}^{DC}$	$\text{T}_{.25}^{SC}$	$\text{T}_{.5}^{SC}$	$\text{T}_{.75}^{SC}$	T^{M}
IMSPE-optimal	$\text{I}_{.25}$	2.1937	0.4306	0.0280	2.0914	0.3936	0.0706	0.6521
	$\text{I}_{.5}$	1.8645	0.3691	0.0268	2.0570	0.4773	0.0754	0.5162
	$\text{I}_{.75}$	2.5201	0.3870	0.0235	2.0880	0.3983	0.0518	0.4609
	I_{M}	2.1269	0.4959	0.0497	2.6889	0.5168	0.0914	0.4108
Space-Filling	MmLHD	2.2112	0.5718	0.0539	2.1850	0.5010	0.0991	0.5291
	mARDLHD	2.1691	0.5681	0.0528	2.7823	0.6478	0.1052	0.5420
W-IMSPE-optimal	$\text{W}_{W}^{.25}$	1.8686	0.4491	0.0296	2.1522	0.4759	0.0691	0.7352
	$\text{W}_{N}^{.25}$	1.8856	0.4150	0.0323	2.0956	0.5543	0.0926	0.5438
	$\text{W}_{N}^{.5}$	1.9562	0.3829	0.0249	2.0010	0.4014	0.0561	0.5133
	W^{U}	2.0548	0.4376	0.0399	2.5183	0.4566	0.0765	0.5093

Table 2 (and Tables 35–37 in Appendix B) show that design choice is more important for small values of $\boldsymbol{\rho}$ than for large values of $\boldsymbol{\rho}$, since the 75$^{\text{th}}$ percentile of EMSPE values becomes smaller and more similar between designs as the test-bed correlation $\boldsymbol{\rho} \to \mathbf{1}$. That is, the values in column $\text{T}_{.25}^{DC}$ are larger and more variable than the values in column $\text{T}_{.5}^{DC}$, and the values in column $\text{T}_{.5}^{DC}$ are larger and more variable than the values in column $\text{T}_{.75}^{DC}$. The same pattern occurs for columns $\text{T}_{.25}^{SC}$, $\text{T}_{.5}^{SC}$, and $\text{T}_{.75}^{SC}$. Surfaces constructed using large values of $\boldsymbol{\rho}$ ($\text{T}_{.75}^{DC}$ and $\text{T}_{.75}^{SC}$) are the easiest to predict because the highly-correlated nature of their outputs results in a relatively flat surface, while surfaces constructed with small values of $\boldsymbol{\rho}$ ($\text{T}_{.25}^{DC}$ and $\text{T}_{.25}^{SC}$) are harder to predict because of the associated $y_{\text{test}}(\cdot)$ variability. A similar observation regarding surface complexity and prediction difficulty was made in Section 4 of Loeppky, Sacks, and Welch (2009).

In order to determine how well a particular design performs across all 7 correlation settings, the designs' 75$^{\text{th}}$ percentiles of EMSPE were standardized within test-bed correlation setting by dividing each design's 75$^{\text{th}}$ percentile by the minimum 75$^{\text{th}}$ percentile seen for that particular correlation setting and design size. Boxplots of the 7 standardized values for the 30×3 designs are given in Figure 4, while Figures 5–7 show the corresponding boxplots for

Figure 4: Boxplots of the seven standardized 75$^{\text{th}}$ percentiles of the 40 EMSPE values, when $(n, d) = (30, 3)$.

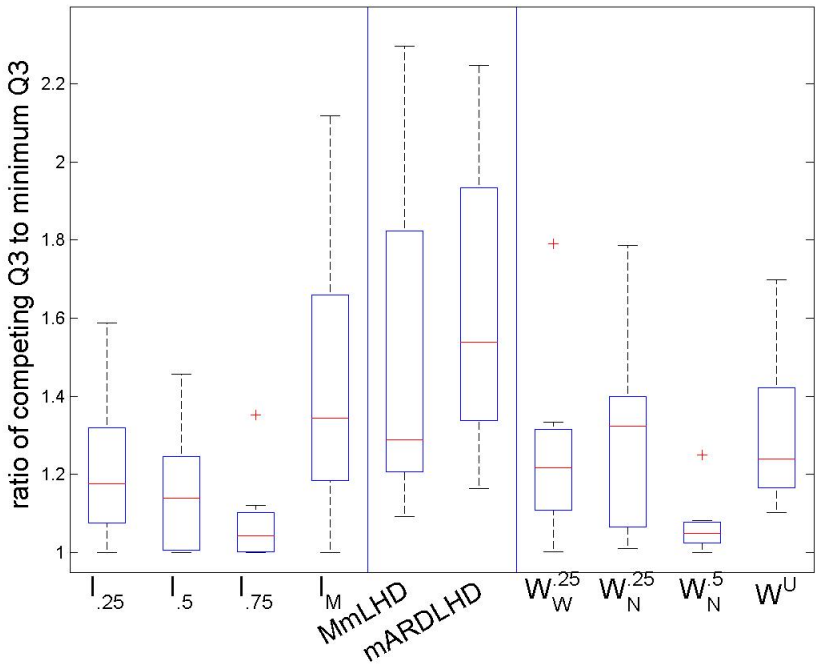

the other design sizes studied. Note that the minimum of the standardized values is 1, and designs having standardized 75$^{\text{th}}$ percentile distributions with values near 1 predict well. Figures 4–7 demonstrate that space-filling designs do not perform as well as the IMSPE- and W-IMSPE-optimal designs across the set of test-bed correlation settings. Therefore, it is recommended that the MmLHD and the mARDLHD should not be used when prediction is the goal of the computer experiment. This recommendation is consistent Pronzato and Müller (2011) and Müller, Pronzato, Rendas, and Waldl (2013) who show that prediction variances are larger for space-filling designs than for competing designs.

Recall that design I_M was constructed for the setting where particular inputs were selected to have high activity and other inputs were specified to have low activity. While I_M also does not perform well across the set of test-bed correlation families, it does predict well for test functions constructed from T^M, the correlation setting for which this design was constructed. Hence, *if the experimenter can specify in advance which simulator inputs have high/low activity*, design I_M is a good choice. However, if the input activity is unclear a priori, it is risky to use design I_M.

Figure 5: Boxplots of the seven standardized 75$^{\text{th}}$ percentiles of the 40 EMSPE values, when $(n, d) = (10, 2)$.

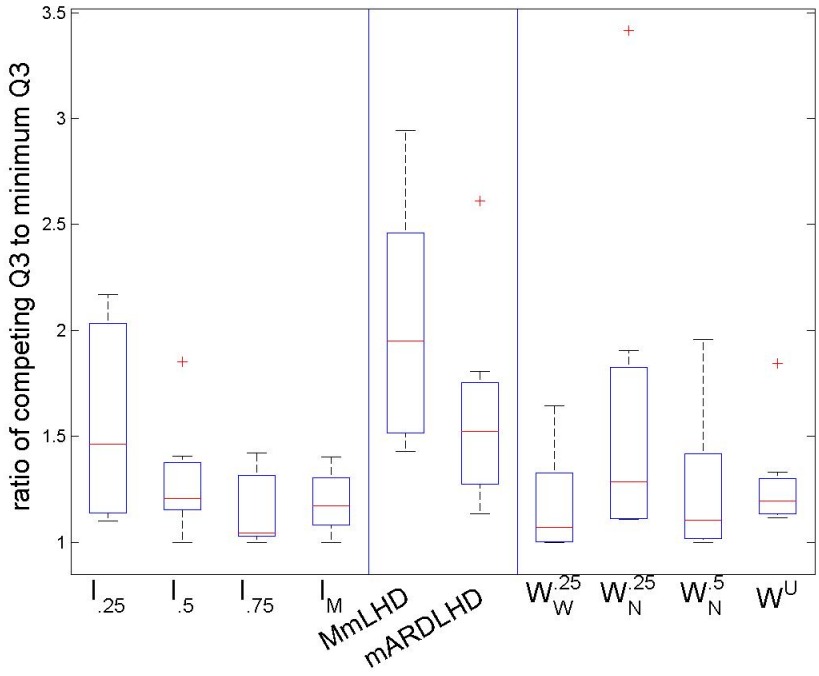

While intuition might suggest the use of designs constructed for the "non-informative" Uniform(0.01, 0.99) weight function when the correlation parameters are unknown, this design does not perform as well across the 7 test-bed correlation families as the other IMSPE- and W-IMSPE-optimal designs.

Instead, Design $\text{I}_{.75}$ is recommended for use in computer experiments when prediction is the experimental goal because of its overall good performance across test-bed correlation families and design sizes. This design is also recommended by Sacks et al. (1989a), for computer experiment designs of size 9×2.

A final set of comparisons will be made, those between the IMSPE- and W-IMSPE-optimal designs. The W-IMSPE-optimal Design $\text{W}_W^{.25}$ generally performs better across the test-bed correlation families than the related IMSPE-optimal design $\text{I}_{.25}$ or the W-IMSPE-optimal design $\text{W}_N^{.25}$. This is true for all design sizes studied but $(n, d) = (16, 5)$. Similarly, the W-IMSPE-optimal design $\text{W}_N^{.5}$ performs similarly or better across the test-bed correlation families than its IMSPE-optimal design $\text{I}_{.5}$. This is true for all design sizes studied except $(n, d) = (10, 2)$. However, the IMSPE-optimal designs take less than 0.5% of the time to

Figure 6: Boxplots of the seven standardized 75^{th} percentiles of the 40 EMSPE values, when $(n, d) = (15, 3)$.

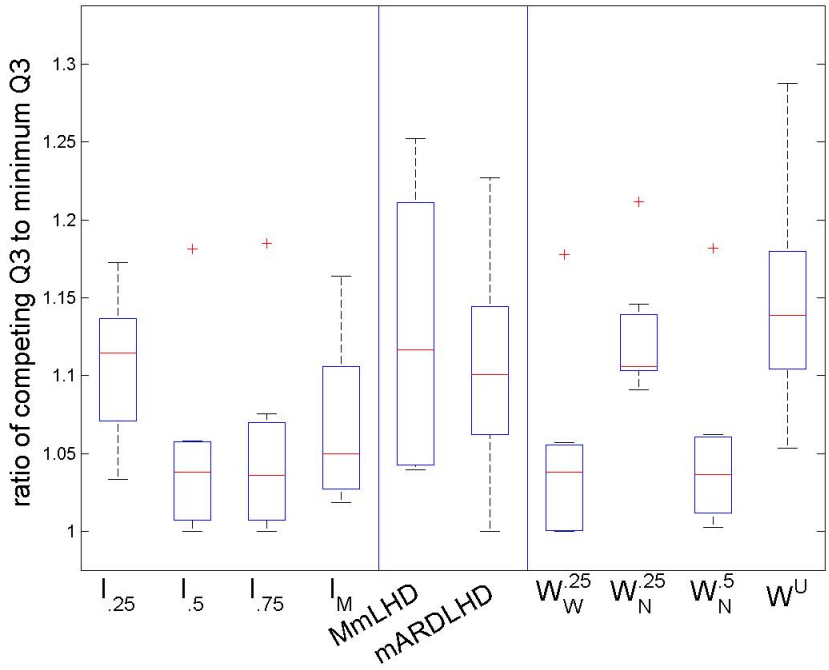

construct than the associated W-IMSPE-optimal designs. Therefore, the experimenter may want to consider paying the price of a slightly larger prediction error in order to use a design that is more rapidly-computable.

7 Summary and Discussion

This paper presents a detailed study of the construction and comparison of initial designs for computer experiments using the minimum weighted integrated mean square prediction error criterion. The minimum W-IMSPE design criterion seeks to identify training data that produce good predictions, on average, over the input space using a prior weight function for the correlation parameters. The minimum W-IMSPE criterion replaces the necessity of determining specific values for correlation parameters in the minimum IMSPE* criterion with that of specifying a $\pi(\boldsymbol{\rho})$ for the GP model correlations. It is shown that two widely-used space-filling designs for computer experiments are inferior to IMSPE- and W-IMSPE-optimal designs with respect to empirical prediction error for a wide range of test functions. Two

Figure 7: Boxplots of the seven standardized 75^{th} percentiles of the 40 EMSPE values, when $(n, d) = (16, 5)$.

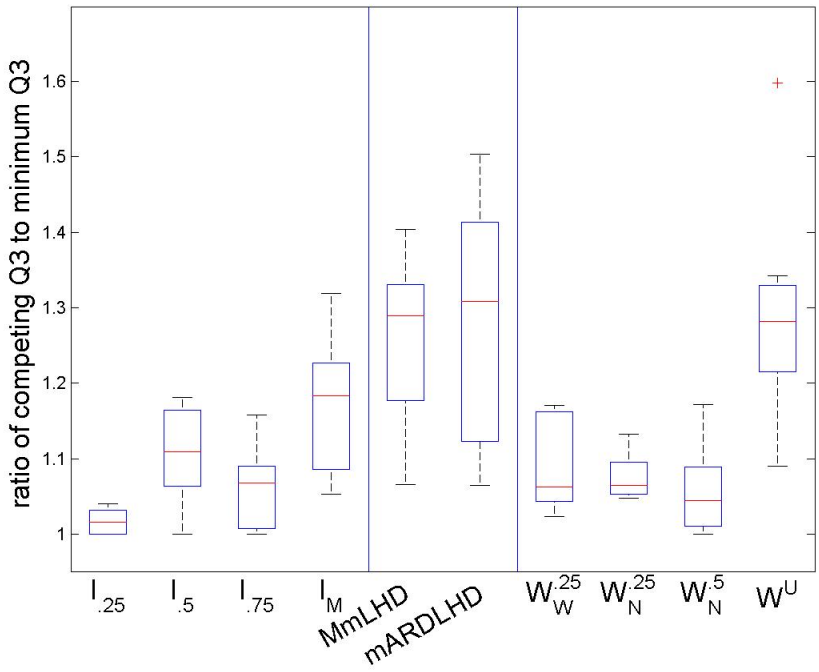

W-IMSPE-optimal designs are recommended as well as a computationally simpler IMSPE-optimal design.

For specific test-bed correlation settings, particular W-IMSPE-optimal designs predicted better than IMSPE-optimal designs, on average, as noted in the previous section. However, the IMSPE-optimal designs take less than 0.5% of the time to construct than the time needed to construct W-IMSPE-optimal designs (see Appendix C for design construction times). Therefore, cost considerations may dictate the use of a rapidly-computable design with slightly larger prediction error. Overall, Design $\text{I}_{.75}$ was found to be the most robust of the rapidly-computable designs investigated, providing good predictions on average, over many surfaces within several test-bed correlation settings. This design is an IMSPE-optimal design constructed assuming correlation values $\boldsymbol{\rho} = 0.75 \times \mathbf{1}_d$.

When physical observations are available, they may be used to *calibrate* the simulator model to obtain simulator output as close as possible to the mean physical response. Currently under investigation are W-IMSPE- and IMSPE-optimal designs for achieving small prediction errors for future physical observations.

The GP model used in this paper is stationary with constant mean. Future work includes examination of designs for prediction using a non-constant mean GP with stationary variance assumption, and eventually to non-stationary models.

ACKNOWLEDGMENTS

This research was sponsored, in part, by an allocation of computing time from the Ohio Supercomputer Center, and by the National Science Foundation under Agreements DMS-0806134 and DMS-1310294 (The Ohio State University). Any opinions, findings, and conclusions or recommendations expressed in this material are those of the author(s) and do not necessarily reflect the views of the National Science Foundation.

SUPPLEMENTARY MATERIAL

Supplementary Material: The supplementary material contains four appendices. Appendix A gives the IMSPE- and W-IMSPE-optimal designs used in the simulation study of Section 6. Appendix B provides tables of the 75^{th} percentiles of the EMSPE values for each combination of design and test-bed correlation setting for $(n, d) \in \{(10, 2), (15, 3), (16, 5)\}$. Appendix C gives the times required to construct the IMSPE- and W-IMSPE-optimal designs for this paper. Lastly, Appendix D lists the space-filling designs used in the simulation study of Section 6. (pdf)

References

Audze, P. and Eglais, V. (1977), "New approach for Planning out of Experiments," *Problems of Dynamics and Strengths*, 35, 104–107.

Bates, R. A., Buck, R. J., Riccomagno, E., and Wynn, H. P. (1996), "Experimental design and observation for large systems," *Journal of the Royal Statistical Society B*, 58, 77–94.

Bates, S. J., Sienz, J., and Toropov, V. V. (2003), "Formulation of the optimal Latin hypercube design of experiments using a permutation genetic algorithm," *Advances in Engineering Software*, 34, 493–506.

Bernardo, M. C., Buck, R. J., Liu, L., Nazaret, W. A., Sacks, J., and Welch, W. J. (1992), "Integrated circuit design optimization using a sequential strategy," *IEEE Transactions on Computer-Aided Design*, 11, 361–372.

Bursztyn, D. and Steinberg, D. M. (2006), "Comparison of designs for computer experiments," *Journal of Statistical Planning and Inference*, 136, 1103–1119.

Currin, C., Mitchell, T. J., Morris, M. D., and Ylvisaker, D. (1991), "Bayesian prediction of deterministic functions, with applications to the design and analysis of computer experiments," *Journal of the American Statistical Association*, 86, 953–963.

Fang, K.-T., Lin, D. K. J., Winker, P., and Zhang, Y. (2000), "Uniform design: theory and application," *Technometrics*, 42, 237–248.

Fogelson, A., Kuharsky, A., and Yu, H. (2003), "Computational Modeling of Blood Clotting: Coagulation and Three-dimensional Platelet Aggregation," in *Polymer and Cell Dynamics: Multicsale Modeling and Numerical Simulations*, Birkhaeuser-Verlag, Basel, pp. 145 – 154.

Forrester, A., Sobester, A., and Keane, A. (2008), *Engineering design via surrogate modelling: a practical guide*, Chichester, UK: Wiley.

Givens, G. and Hoeting, J. (2012), *Computational Statistics*, Wiley.

Hajagos, J. G. (2005), "Modeling Uncertainty in Population Biology: How the Model is Written Does Matter," in *Proceedings of the SAMO 2004 Conference on Sensitivity Analysis*, eds. Hanson, K. M. and Hemez, F. M., Los Alamos National Laboratory, Los Alamos: http://library.lanl.gov/ccw/samo2004/, pp. 363–368.

Hayeck, G. T. (2009), "The kinematics of the upper extremity and subsequent effects on joint loading and surgical treatment," Ph.D. thesis, Cornell University, Ithaca, NY USA.

Higdon, D., Kennedy, M., Cavendish, J., Cafeo, J., and Ryne, R. (2004), "Combining field data and computer simulations for calibration and prediction," *SIAM Journal of Scientific Computing*, 26, 448–466.

Johnson, M. E., Moore, L. M., and Ylvisaker, D. (1990), "Minimax and maximin distance designs," *Journal of Statistical Planning and Inference*, 26, 131–148.

Johnson, R., Jones, B., Fowler, J., and Montgomery, D. (2008), "Comparing designs for computer simulation experiments," in *Simulation Conference, 2008. WSC 2008. Winter*, pp. 463–470.

Jones, D. R., Schonlau, M., and Welch, W. J. (1998), "Efficient global optimization of expensive black–box functions," *Journal of Global Optimization*, 13, 455–492.

Kennedy, J. and Eberhart, R. (1995), "Particle swarm optimization," in *Neural Networks, 1995. Proceedings., IEEE International Conference on*, vol. 4, pp. 1942–1948.

Kincaid, D. and Cheney, E. (2002), *Numerical Analysis: Mathematics of Scientific Computing*, American Mathematical Society.

Koehler, J. R. and Owen, A. B. (1996), "Computer experiments," in *Handbook of Statistics*, eds. Ghosh, S. and Rao, C. R., Elsevier Science B.V., vol. 13, pp. 261–308.

Leatherman, E., Dean, A., and Santner, T. (2014), "Computer Experiment Designs via Particle Swarm Optimization," Submitted.

Lempert, R., Schlensinger, M. E., Bankes, S., and Andronova, N. (2000), "The impacts of climate variability on near-term policy choices and the value of information," *Climate Change*, 45, 129–161.

Liefvendahl, M. and Stocki, R. (2006), "A study on algorithms for optimization of Latin hypercubes," *Journal of Statistical Planning and Inference*, 136, 3231–3247.

Loeppky, J. L., Sacks, J., and Welch, W. J. (2009), "Choosing the Sample Size of a Computer Experiment: A Practical Guide," *Technometrics*, 51, 366–376.

MATLAB Parametric Empirical Kriging (MPErK) (2013), T.J. Santner Group, The Ohio State University.

McKay, M. D., Beckman, R. J., and Conover, W. J. (1979), "A comparison of three methods for selecting values of input variables in the analysis of output from a computer code," *Technometrics*, 21, 239–245.

Mitchell, T. J. and Scott, D. S. (1987), "A computer program for the design of group testing experiments," *Communications in Statistics - Theory and Methods*, 16, 2943–2955.

Morokoff, W. J. and Caflisch, R. E. (1995), "Quasi-Monte Carlo Integration," *Journal of Computational Physics*, 122, 218–230.

Morris, M. D. and Mitchell, T. J. (1995), "Exploratory designs for computational experiments," *Journal of Statistical Planning and Inference*, 43, 381–402.

Müller, W., Pronzato, L., Rendas, J., and Waldl, H. (2013), "Efficient Prediction Designs for Random Fields," Tech. rep., Department for Applied Statistics, Johannes Kepler University Linz, iFAS Research Paper Series 2013–63.

Nekkanty, S. (2009), "Characterization of damage and optimization of thin film coatings on ductile substrates." Ph.D. thesis, Department of Mechanical Engineering, The Ohio State University, Columbus, Ohio, USA.

Niederreiter, H. (1992), *Random Number Generation and Quasi-Monte Carlo Methods*, Philadelphia: SIAM.

Ong, K., Santner, T., and Bartel, D. (2008), "Robust Design for Acetabular Cup Stability Accounting for Patient and Surgical Variability,," *Journal of Biomechanical Engineering*, 130, 031001.

Pronzato, L. and Müller, W. (2011), "Design of computer experiments: space filling and beyond," *Statistics and Computing*, 1–21, 10.1007/s11222-011-9242-3.

Sacks, J., Schiller, S. B., and Welch, W. J. (1989a), "Design for computer experiments," *Technometrics*, 31, 41–47.

Sacks, J., Welch, W. J., Mitchell, T. J., and Wynn, H. P. (1989b), "Design and analysis of computer experiments," *Statistical Science*, 4, 409–423.

Santner, T. J., Williams, B. J., and Notz, W. I. (2003), *The Design and Analysis of Computer Experiments*, New York: Springer Verlag.

Shewry, M. C. and Wynn, H. P. (1987), "Maximum entropy sampling," *Journal of Applied Statistics*, 14, 165–170.

Specht, E. (2013), "Packomania.com," `http://www.packomania.com/`, accessed: April 2013.

Trosset, M. W. (1999), "The krigifier: a procedure for generating pseudorandom nonlinear objective functions for computational experimentation," Tech. Rep. 35, Institute for Computer Applications in Science and Engineering, NASA Langley Research Center.

Upton, M. L., Guilak, F., Laursen, T. A., and Setton, L. A. (2006), "Finite Element Modeling Predictions of Region-specific Cell-matrix Mechanics in the Meniscus," *Biomechanics and Modeling in Mechanobiology*, 5, 140–149.

van Dam, E., den Hertog, D., Husslage, B., and Rennen, G. (2013), "Space-filling designs," `http://www.spacefillingdesigns.nl/`, accessed: March 2013.

Wang, Y. and Fang, K.-T. (1981), "A note on uniform distribution and experimental design," *Kexue Tongbao (Chinese Science Bulletin)*, 26, 485–489.

Yang, X.-S. (2010), *Engineering Optimization: An Introduction with Metaheuristic Applications*, Wiley Publishing, 1st ed.

Supplementary Material

The supplementary material contains four appendices. Appendix A gives the IMSPE- and W-IMSPE-optimal designs used in the simulation study of Section 6. Appendix B provides tables of the 75^{th} percentiles of the EMSPE values for each combination of design and test-bed correlation setting for $(n, d) \in \{(10, 2), (15, 3), (16, 5)\}$. Appendix C gives the times required to construct the IMSPE- and W-IMSPE-optimal designs for this paper. Lastly, Appendix D lists the space-filling designs used in the simulation study of Section 6.

A IMSPE- and W-IMSPE-optimal Designs

Table 3: A 10-run IMSPE-optimal design in $[0, 1]^2$ for prior $\mathrm{I}_{.25}$. This design was constructed using $N_{\text{des}} = 80 = 4 \times n \times d$ designs (particles) and $N_{\text{its}} = 160 = 2 \times N_{\text{des}}$ iterations for PSO. The IMSPE* value of this design is 0.0464.

x_1	x_2
0.1438	0.1398
0.5109	0.9161
0.8497	0.5016
0.4971	0.3407
0.1397	0.4996
0.5049	0.0840
0.8612	0.1421
0.1444	0.8611
0.4910	0.6597
0.8621	0.8579

Table 4: A 10-run IMSPE-optimal design in $[0,1]^2$ for prior $\mathrm{I}_{.5}$. This design was constructed using $N_{\text{des}} = 80 = 4 \times n \times d$ designs (particles) and $N_{\text{its}} = 160 = 2 \times N_{\text{des}}$ iterations for PSO. The IMSPE* value of this design is 0.0082.

x_1	x_2
0.1514	0.8880
0.9140	0.8683
0.8231	0.5425
0.1535	0.1328
0.3570	0.6216
0.5615	0.0599
0.0698	0.5033
0.5002	0.3157
0.8994	0.1622
0.5787	0.8776

Table 5: A 10-run IMSPE-optimal design in $[0,1]^2$ for prior $\mathrm{I}_{.75}$. This design was constructed using $N_{\text{des}} = 80 = 4 \times n \times d$ designs (particles) and $N_{\text{its}} = 160 = 2 \times N_{\text{des}}$ iterations for PSO. The IMSPE* value of this design is 5.2025×10^{-4}.

x_1	x_2
0.5573	0.0627
0.1674	0.9105
0.7432	0.4034
0.3078	0.3977
0.1272	0.1336
0.9384	0.7220
0.5071	0.7739
0.0431	0.5924
0.9017	0.1568
0.7772	1.0000

Table 6: A 10-run W-IMSPE-optimal design in $[0,1]^2$ for prior W_W^{25}. This design was constructed using 2^{11} Sobol´ draws for $N_{\text{des}} = 80 = 4 \times n \times d$ designs (particles) and $N_{\text{its}} = 240 = 3 \times N_{\text{des}}$ iterations for PSO. The W-IMSPE value of this design is 0.0013.

x_1	x_2
0.1732	0.9239
0.8065	0.9327
0.9397	0.6606
0.1167	0.1399
0.0675	0.6220
0.5165	0.0650
0.3027	0.3758
0.7177	0.4060
0.8914	0.1460
0.4873	0.7779

Table 7: A 10-run W-IMSPE-optimal design in $[0,1]^2$ for prior W_N^{25}. This design was constructed using 2^{11} Sobol´ draws for $N_{\text{des}} = 80 = 4 \times n \times d$ designs (particles) and $N_{\text{its}} = 240 = 3 \times N_{\text{des}}$ iterations for PSO. The W-IMSPE value of this design is 0.0974.

x_1	x_2
0.1285	0.8725
0.8500	0.8656
0.8903	0.4822
0.1341	0.1498
0.6220	0.5814
0.5172	0.1119
0.1365	0.5453
0.4118	0.3804
0.8533	0.1470
0.4564	0.8610

Table 8: A 10-run W-IMSPE-optimal design in $[0,1]^2$ for prior W_N^5. This design was constructed using 2^{11} Sobol´ draws for $N_{\text{des}} = 80 = 4 \times n \times d$ designs (particles) and $N_{\text{its}} = 240 = 3 \times N_{\text{des}}$ iterations for PSO. The W-IMSPE value of this design is 0.0175.

x_1	x_2
0.8908	0.1535
0.3314	0.5695
0.0692	0.5148
0.5602	0.3291
0.1481	0.1450
0.8511	0.5602
0.5619	0.8552
0.1521	0.8900
0.5183	0.0679
0.8964	0.8935

Table 9: A 10-run W-IMSPE-optimal design in $[0,1]^2$ for prior W^U. This design was constructed using 2^{11} Sobol´ draws for $N_{\text{des}} = 80 = 4 \times n \times d$ designs (particles) and $N_{\text{its}} = 160 = 2 \times N_{\text{des}}$ iterations for PSO. The W-IMSPE value of this design is 0.0243.

x_1	x_2
0.8249	0.1168
0.3332	0.0784
0.5684	0.2985
0.9164	0.4641
0.4265	0.9143
0.0852	0.2553
0.2664	0.5292
0.8608	0.8685
0.1037	0.8088
0.6405	0.6680

Table 10: A 10-run IMSPE-optimal design in $[0,1]^2$ for prior I_M. This design was constructed using $N_{\text{des}} = 80 = 4 \times n \times d$ designs (particles) and $N_{\text{its}} = 160 = 2 \times N_{\text{des}}$ iterations for PSO. The IMSPE* value of this design is 0.0078.

x_1	x_2
0.1083	0.8388
0.3816	0.0395
0.5223	0.2906
0.8906	0.8589
0.4764	0.9621
0.1848	0.5167
0.8654	0.1280
0.8512	0.4864
0.0897	0.1967
0.5570	0.7124

Table 11: A 15-run IMSPE-optimal design in $[0,1]^3$ for prior $\mathrm{I}_{.25}$. This design was constructed using $N_{\text{des}} = 180 = 4 \times n \times d$ designs (particles) and $N_{\text{its}} = 360 = 2 \times N_{\text{des}}$ iterations for PSO. The IMSPE* value of this design is 0.1982.

x_1	x_2	x_3
0.8097	0.8163	0.8140
0.7695	0.2290	0.1319
0.4628	0.5368	0.8298
0.1838	0.1900	0.1861
0.4637	0.5351	0.1703
0.7702	0.2309	0.8689
0.4767	0.1784	0.5008
0.8095	0.8156	0.1857
0.1763	0.8235	0.1903
0.1762	0.8240	0.8085
0.8704	0.1294	0.5009
0.1610	0.5049	0.4999
0.4944	0.8386	0.4993
0.1839	0.1904	0.8143
0.8213	0.5227	0.5000

Table 12: A 15-run IMSPE-optimal design in $[0,1]^3$ for prior $\mathrm{I}_{.5}$. This design was constructed using $N_{\mathrm{des}} = 180 = 4 \times n \times d$ designs (particles) and $N_{\mathrm{its}} = 360 = 2 \times N_{\mathrm{des}}$ iterations for PSO. The IMSPE* value of this design is 0.0539.

x_1	x_2	x_3
0.8551	0.4992	0.4909
0.8392	0.8199	0.1592
0.1763	0.8260	0.1671
0.5143	0.5014	0.8459
0.1543	0.5009	0.4866
0.2198	0.8861	0.7831
0.8385	0.1789	0.1605
0.2163	0.1162	0.7836
0.1158	0.5044	0.8834
0.5449	0.8556	0.4549
0.8332	0.8266	0.8231
0.1755	0.1743	0.1681
0.8321	0.1727	0.8235
0.5447	0.1452	0.4545
0.5052	0.4991	0.1458

Table 13: A 15-run IMSPE-optimal design in $[0,1]^3$ for prior $\mathrm{I}_{.75}$. This design was constructed using $N_{\mathrm{des}} = 180 = 4 \times n \times d$ designs (particles) and $N_{\mathrm{its}} = 360 = 2 \times N_{\mathrm{des}}$ iterations for PSO. The IMSPE* value of this design is 0.0062.

x_1	x_2	x_3
0.8400	0.8513	0.1612
0.4214	0.5269	0.8780
0.1446	0.8604	0.8276
0.4922	0.1247	0.5037
0.1581	0.1609	0.1507
0.1448	0.8523	0.1676
0.1591	0.1528	0.8337
0.8718	0.5152	0.4896
0.8854	0.1095	0.5206
0.1283	0.4898	0.5148
0.8010	0.2011	0.8979
0.8341	0.8461	0.8487
0.8063	0.1926	0.1021
0.4884	0.8698	0.5027
0.4778	0.5524	0.1229

Table 14: A 15-run W-IMSPE-optimal design in $[0,1]^3$ for prior W_W^{25}. This design was constructed using $N_{\text{des}} = 180 = 4 \times n \times d$ designs (particles) and $N_{\text{its}} = 360 = 2 \times N_{\text{des}}$ iterations for PSO. The first 90% of the iterations were based on 2^{11} Sobol´ draws, and the final iterations were based on 2^{16} Sobol´ draws. The W-IMSPE value of this design is 0.2275.

x_1	x_2	x_3
0.8781	0.8767	0.4999
0.8136	0.1818	0.1842
0.1823	0.8132	0.8165
0.4947	0.1568	0.4999
0.8231	0.4769	0.5007
0.1749	0.1742	0.1866
0.8126	0.1819	0.8169
0.7711	0.7708	0.1340
0.1820	0.8132	0.1834
0.1559	0.4948	0.4996
0.4659	0.4661	0.8311
0.4667	0.4659	0.1680
0.4775	0.8231	0.4992
0.1748	0.1744	0.8132
0.7705	0.7709	0.8659

Table 15: A 15-run W-IMSPE-optimal design in $[0,1]^3$ for prior W_N^{25}. This design was constructed using $N_{\text{des}} = 180 = 4 \times n \times d$ designs (particles) and $N_{\text{its}} = 360 = 2 \times N_{\text{des}}$ iterations for PSO. The first 90% of the iterations were based on 2^{11} Sobol´ draws, and the final iterations were based on 2^{16} Sobol´ draws. The W-IMSPE value of this design is 0.6197.

x_1	x_2	x_3
0.8299	0.8554	0.4995
0.6530	0.2056	0.1319
0.1783	0.6309	0.8479
0.4689	0.1224	0.4999
0.4909	0.5155	0.4999
0.1687	0.2035	0.2338
0.8802	0.2206	0.5012
0.8483	0.6057	0.1665
0.5176	0.8525	0.1769
0.1707	0.8397	0.5002
0.6507	0.2062	0.8686
0.1775	0.6301	0.1527
0.5186	0.8531	0.8227
0.1676	0.2043	0.7646
0.8485	0.6060	0.8336

Table 16: A 15-run W-IMSPE-optimal design in $[0,1]^3$ for prior W_N^5. This design was constructed using $N_{\text{des}} = 180 = 4 \times n \times d$ designs (particles) and $N_{\text{its}} = 360 = 2 \times N_{\text{des}}$ iterations for PSO. The first 90% of the iterations were based on 2^{11} Sobol´ draws, and the final iterations were based on 2^{16} Sobol´ draws. The W-IMSPE value of this design is 0.1596.

x_1	x_2	x_3
0.5449	0.8550	0.4552
0.8396	0.1785	0.1603
0.1126	0.5007	0.8872
0.5445	0.1450	0.4557
0.5151	0.5001	0.8450
0.1749	0.1733	0.1682
0.8553	0.5000	0.4944
0.8397	0.8212	0.1602
0.1749	0.8266	0.1681
0.1553	0.5001	0.4845
0.8322	0.1734	0.8249
0.5050	0.4999	0.1444
0.2173	0.8831	0.7829
0.2170	0.1171	0.7833
0.8323	0.8266	0.8248

Table 17: A 15-run W-IMSPE-optimal design in $[0,1]^3$ for prior W^U. This design was constructed using $N_{\text{des}} = 180 = 4 \times n \times d$ designs (particles) and $N_{\text{its}} = 360 = 2 \times N_{\text{des}}$ iterations for PSO. The first 90% of the iterations were based on 2^{11} Sobol´ draws, and the final iterations were based on 2^{16} Sobol´ draws. The W-IMSPE value of this design is 0.0951.

x_1	x_2	x_3
0.7964	0.8769	0.4274
0.6021	0.1928	0.1231
0.2409	0.5448	0.8942
0.2960	0.1025	0.3992
0.6524	0.4144	0.6257
0.1279	0.4103	0.1673
0.8854	0.1665	0.4732
0.8618	0.5721	0.1362
0.3478	0.8672	0.1217
0.1196	0.8071	0.5444
0.5996	0.1454	0.8737
0.4603	0.6076	0.3566
0.5004	0.8851	0.8107
0.1160	0.2057	0.7281
0.8814	0.6426	0.8422

Table 18: A 15-run IMSPE-optimal design in $[0,1]^3$ for prior I_M. This design was constructed using $N_{\mathrm{des}} = 180 = 4 \times n \times d$ designs (particles) and $N_{\mathrm{its}} = 360 = 2 \times N_{\mathrm{des}}$ iterations for PSO. The IMSPE* value of this design is 0.0863.

x_1	x_2	x_3
0.1832	0.2630	0.1699
0.2885	0.9077	0.5137
0.7712	0.7156	0.4609
0.1968	0.7560	0.8746
0.7111	0.0991	0.1458
0.7630	0.8898	0.8289
0.7254	0.4994	0.1233
0.2431	0.5000	0.5459
0.2868	0.0923	0.5151
0.1837	0.7370	0.1706
0.7257	0.5003	0.8417
0.7102	0.9002	0.1448
0.7713	0.2853	0.4601
0.7639	0.1104	0.8294
0.1972	0.2449	0.8750

Table 19: A 30-run IMSPE-optimal design in $[0,1]^3$ for prior $\mathrm{I}_{.25}$. This design was constructed using $N_{\mathrm{des}} = 360 = 4 \times n \times d$ designs (particles) and $N_{\mathrm{its}} = 720 = 2 \times N_{\mathrm{des}}$ iterations for PSO. The IMSPE* value of this design is 0.0640.

x_1	x_2	x_3
0.4994	0.8186	0.9048
0.6724	0.6423	0.6180
0.5008	0.4617	0.0714
0.1198	0.5758	0.1572
0.3242	0.6467	0.6165
0.4969	0.3891	0.8373
0.1466	0.0968	0.4551
0.4989	0.1531	0.6104
0.8812	0.8452	0.4241
0.5028	0.7686	0.2358
0.1459	0.1605	0.8378
0.1372	0.1789	0.1124
0.8522	0.0963	0.4556
0.3276	0.3816	0.3629
0.1493	0.5429	0.9054
0.5015	0.9302	0.5424
0.8541	0.1602	0.8371
0.7832	0.8943	0.1028
0.5000	0.0959	0.1805
0.1361	0.8864	0.8232
0.2210	0.8948	0.1027
0.8802	0.5732	0.1585
0.5004	0.1013	0.9051
0.0866	0.4411	0.5624
0.8621	0.1772	0.1128
0.1191	0.8465	0.4230
0.8473	0.5384	0.9061
0.6731	0.3784	0.3640
0.8641	0.8839	0.8234
0.9136	0.4417	0.5645

Table 20: A 30-run IMSPE-optimal design in $[0,1]^3$ for prior $\mathrm{I}_{.5}$. This design was constructed using $N_{\mathrm{des}} = 360 = 4 \times n \times d$ designs (particles) and $N_{\mathrm{its}} = 720 = 2 \times N_{\mathrm{des}}$ iterations for PSO. The IMSPE* value of this design is 0.0094.

x_1	x_2	x_3
0.8621	0.8683	0.8390
0.6541	0.3197	0.3814
0.4663	0.8572	0.9213
0.3335	0.6891	0.5945
0.3389	0.3212	0.6069
0.0625	0.4989	0.5878
0.1024	0.8804	0.8433
0.1816	0.4952	0.2300
0.8936	0.5010	0.6333
0.5521	0.9260	0.5860
0.5109	0.4985	0.0608
0.9250	0.5016	0.1581
0.8852	0.4945	0.9355
0.1254	0.8984	0.4052
0.0998	0.8041	0.0716
0.9139	0.8784	0.4061
0.4133	0.8953	0.1632
0.6495	0.5091	0.8274
0.5473	0.0722	0.5864
0.1787	0.5033	0.9266
0.8215	0.1343	0.0871
0.8575	0.1295	0.8373
0.4689	0.1515	0.9226
0.9135	0.1223	0.4113
0.1056	0.1197	0.8459
0.1002	0.1885	0.0754
0.8208	0.8652	0.0851
0.1280	0.1026	0.4099
0.6514	0.6806	0.3710
0.4167	0.1060	0.1657

Table 21: A 30-run IMSPE-optimal design in $[0,1]^3$ for prior $\mathrm{I}_{.75}$. This design was constructed using $N_{\mathrm{des}} = 360 = 4 \times n \times d$ designs (particles) and $N_{\mathrm{its}} = 720 = 2 \times N_{\mathrm{des}}$ iterations for PSO. The IMSPE* value of this design is 5.3755×10^{-4}.

x_1	x_2	x_3
1.0000	0.1116	0.5233
0.0000	0.3229	0.3762
0.1088	0.1072	0.1033
0.5256	0.7503	0.6855
0.6749	0.0974	0.7911
0.8021	0.8993	0.4272
0.6928	0.0000	0.1457
0.6727	0.9590	1.0000
0.7099	0.6058	0.1155
0.3106	0.1447	0.9287
0.5836	0.5822	1.0000
0.0000	0.7762	0.5924
0.0000	0.0908	0.7914
0.3385	0.0000	0.4428
0.0949	0.9013	0.1630
0.3522	0.9159	0.5174
0.1731	0.9071	0.8945
1.0000	0.8360	0.8243
0.4612	0.2664	0.0994
0.4886	0.9377	0.0002
0.2935	0.3849	0.7047
0.3823	0.6633	0.3510
0.1269	0.5000	0.8985
0.6149	0.3068	0.3780
0.1461	0.5513	0.0782
0.8523	0.4698	0.7989
0.9417	0.5511	0.3998
1.0000	0.2311	0.0911
0.9207	0.1529	1.0000
1.0000	0.9005	0.0000

Table 22: A 30-run W-IMSPE-optimal design in $[0,1]^3$ for prior W_W^{25}. This design was constructed using $N_{\text{des}} = 360 = 4 \times n \times d$ designs (particles) and $N_{\text{its}} = 720 = 2 \times N_{\text{des}}$ iterations for PSO. The first 90% of the iterations were based on 2^{11} Sobol´ draws, and the final iterations were based on 2^{16} Sobol´ draws. The W-IMSPE value of this design is 0.0749.

x_1	x_2	x_3
0.4412	0.8924	0.8498
0.2858	0.5643	0.7184
0.1759	0.9000	0.5456
0.3952	0.6919	0.3582
0.5957	0.5617	0.1080
0.1283	0.1168	0.6161
0.5441	0.0745	0.4546
0.8359	0.1274	0.1512
0.8457	0.8592	0.1468
0.9155	0.7345	0.4924
0.3623	0.1067	0.8797
0.1221	0.1275	0.1901
0.9065	0.1695	0.5381
0.4428	0.8900	0.1257
0.1083	0.3288	0.8872
0.0745	0.5225	0.4688
0.9005	0.4618	0.8335
0.6537	0.9169	0.4776
0.4642	0.1748	0.1000
0.1095	0.7954	0.8786
0.1785	0.4786	0.0985
0.3242	0.3166	0.3831
0.8068	0.1198	0.8789
0.5717	0.2926	0.6980
0.9108	0.4769	0.1445
0.1079	0.8404	0.1654
0.6584	0.6626	0.6479
0.5392	0.5230	0.9315
0.8484	0.8598	0.8560
0.7267	0.4099	0.3683

Table 23: A 30-run W-IMSPE-optimal design in $[0,1]^3$ for prior $\mathrm{W}_N^{.25}$. This design was constructed using $N_{\mathrm{des}} = 360 = 4 \times n \times d$ designs (particles) and $N_{\mathrm{its}} = 720 = 2 \times N_{\mathrm{des}}$ iterations for PSO. The first 90% of the iterations were based on 2^{11} Sobol´ draws, and the final iterations were based on 2^{16} Sobol´ draws. The W-IMSPE value of this design is 0.1941.

x_1	x_2	x_3
0.4540	0.8512	0.9042
0.3607	0.6748	0.6237
0.5670	0.9155	0.5613
0.1565	0.8838	0.4233
0.2464	0.5007	0.2453
0.3604	0.3253	0.6240
0.1565	0.1162	0.4236
0.5673	0.0843	0.5616
0.8215	0.8635	0.1145
0.9051	0.4996	0.1789
0.6110	0.5004	0.8469
0.1043	0.2306	0.1066
0.9058	0.5000	0.8999
0.4213	0.8838	0.1538
0.1794	0.5002	0.9052
0.0711	0.5001	0.5378
0.8375	0.1464	0.8394
0.5378	0.4990	0.0701
0.4204	0.1158	0.1539
0.1131	0.8624	0.8206
0.6226	0.6742	0.3548
0.6206	0.3248	0.3552
0.4539	0.1492	0.9043
0.1131	0.1378	0.8207
0.8210	0.1357	0.1148
0.1044	0.7700	0.1063
0.8375	0.5001	0.6119
0.8376	0.8536	0.8392
0.9066	0.8466	0.4570
0.9067	0.1539	0.4574

Table 24: A 30-run W-IMSPE-optimal design in $[0,1]^3$ for prior $\mathrm{W}_N^{\cdot 5}$. This design was constructed using $N_{\text{des}} = 360 = 4 \times n \times d$ designs (particles) and $N_{\text{its}} = 720 = 2 \times N_{\text{des}}$ iterations for PSO. The first 90% of the iterations were based on 2^{11} Sobol´ draws, and the final iterations were based on 2^{16} Sobol´ draws. The W-IMSPE value of this design is 0.0289.

x_1	x_2	x_3
0.3616	0.3261	0.3369
0.8948	0.1205	0.5699
0.6656	0.3149	0.6043
0.9052	0.4884	0.3575
0.8364	0.1384	0.9094
0.9126	0.8659	0.5720
0.4826	0.1944	0.0807
0.1059	0.1897	0.9140
0.9227	0.5125	0.8355
0.8656	0.8704	0.1536
0.8208	0.8744	0.9035
0.1205	0.1237	0.1470
0.6266	0.6915	0.6755
0.5265	0.4880	0.9399
0.3014	0.7001	0.4124
0.0583	0.4833	0.4407
0.5322	0.0702	0.3789
0.6630	0.5802	0.2361
0.2365	0.4418	0.7404
0.1030	0.8860	0.1686
0.1316	0.0964	0.5843
0.3739	0.9065	0.8738
0.8638	0.1249	0.1514
0.4548	0.8530	0.0772
0.0920	0.7278	0.9117
0.4354	0.0951	0.8335
0.5458	0.9362	0.4370
0.8419	0.5006	0.0750
0.1633	0.5273	0.0733
0.1132	0.9052	0.6283

Table 25: A 30-run W-IMSPE-optimal design in $[0,1]^3$ for prior W^U. This design was constructed using $N_{\text{des}} = 360 = 4 \times n \times d$ designs (particles) and $N_{\text{its}} = 720 = 2 \times N_{\text{des}}$ iterations for PSO. The first 90% of the iterations were based on 2^{11} Sobol´ draws, and the final iterations were based on 2^{16} Sobol´ draws. The W-IMSPE value of this design is 0.0272.

x_1	x_2	x_3
0.4949	0.8672	0.9182
0.3613	0.6693	0.7289
0.0801	0.2349	0.7693
0.0989	0.6251	0.4611
0.2906	0.0997	0.1056
0.3395	0.3740	0.5437
0.1525	0.0753	0.4665
0.5166	0.1803	0.3209
0.9168	0.4570	0.6634
0.2190	0.5922	0.0739
0.6094	0.4052	0.8656
0.0750	0.3206	0.2089
0.6367	0.6433	0.4956
0.3333	0.9230	0.4966
0.1691	0.5214	0.9202
0.4318	0.7538	0.2424
0.8522	0.1791	0.8884
0.7928	0.3683	0.3234
0.5491	0.4201	0.0773
0.1030	0.8747	0.7915
0.6759	0.9018	0.1147
0.9049	0.6088	0.1174
0.6269	0.0889	0.6627
0.3557	0.1071	0.9047
0.8078	0.1337	0.1167
0.1174	0.8937	0.1812
0.8867	0.7070	0.9065
0.7668	0.9235	0.7156
0.9109	0.8618	0.3895
0.9222	0.1043	0.4517

Table 26: A 30-run IMSPE-optimal design in $[0,1]^3$ for prior I_M. This design was constructed using $N_{\mathrm{des}} = 360 = 4 \times n \times d$ designs (particles) and $N_{\mathrm{its}} = 720 = 2 \times N_{\mathrm{des}}$ iterations for PSO. The IMSPE* value of this design is 0.0184.

x_1	x_2	x_3
0.4898	0.7803	0.6707
0.9063	0.2887	0.4747
0.3301	0.6472	0.9313
0.1416	0.3293	0.4456
0.1250	0.6010	0.6821
0.7797	0.4139	0.9380
0.8214	0.9057	0.0935
0.6243	0.8840	0.3221
0.5511	0.3316	0.2568
0.6027	0.5459	0.4840
0.8332	0.9222	0.5886
0.1779	0.0986	0.6764
0.1602	0.6729	0.3301
0.9096	0.6575	0.2908
0.3516	0.0873	0.9277
0.8931	0.6121	0.7406
0.7645	0.8727	0.9073
0.7349	0.0755	0.5198
0.8170	0.3830	0.0706
0.5737	0.6705	0.0917
0.8482	0.1189	0.8410
0.2560	0.1367	0.0801
0.7897	0.0887	0.1500
0.1553	0.4712	0.0954
0.5362	0.3265	0.7059
0.1940	0.8879	0.1108
0.2233	0.0776	0.3376
0.2044	0.9051	0.8709
0.1807	0.9344	0.4989
0.1547	0.3408	0.8879

Table 27: A 16-run IMSPE-optimal design in $[0,1]^5$ for prior $\mathrm{I}_{.25}$. This design was constructed using $N_{\text{des}} = 320 = 4 \times n \times d$ designs (particles) and $N_{\text{its}} = 640 = 2 \times N_{\text{des}}$ iterations for PSO. The IMSPE* value of this design is 0.6935.

x_1	x_2	x_3	x_4	x_5
0.2617	0.2608	0.2612	0.2617	0.7396
0.7397	0.7374	0.7385	0.2615	0.2613
0.2616	0.2606	0.2603	0.7367	0.2605
0.7397	0.7384	0.2604	0.7372	0.2616
0.7386	0.2606	0.7400	0.2635	0.7388
0.7390	0.7390	0.2628	0.2607	0.7395
0.2606	0.7378	0.7389	0.2606	0.7381
0.2609	0.7391	0.7375	0.7381	0.2604
0.7383	0.2618	0.7376	0.7404	0.2612
0.7398	0.2610	0.2625	0.2604	0.2632
0.2621	0.2608	0.7379	0.2608	0.2612
0.2597	0.2617	0.7378	0.7390	0.7377
0.2609	0.7384	0.2616	0.7395	0.7386
0.7395	0.2618	0.2618	0.7391	0.7389
0.2621	0.7383	0.2609	0.2602	0.2613
0.7376	0.7393	0.7388	0.7385	0.7387

Table 28: A 16-run IMSPE-optimal design in $[0,1]^5$ for prior $\mathrm{I}_{.5}$. This design was constructed using $N_{\mathrm{des}} = 320 = 4 \times n \times d$ designs (particles) and $N_{\mathrm{its}} = 640 = 2 \times N_{\mathrm{des}}$ iterations for PSO. The IMSPE* value of this design is 0.3752.

x_1	x_2	x_3	x_4	x_5
0.2680	0.7327	0.7328	0.7466	0.2673
0.7568	0.2435	0.7149	0.7563	0.2857
0.2673	0.7327	0.7320	0.2671	0.7467
0.2842	0.7162	0.2432	0.7571	0.7567
0.7566	0.2422	0.2435	0.2841	0.2844
0.7572	0.7147	0.2430	0.2852	0.7579
0.7562	0.2440	0.7164	0.2842	0.7563
0.7561	0.7155	0.7163	0.7561	0.7564
0.2677	0.2535	0.7328	0.2673	0.2674
0.2838	0.2431	0.2435	0.7569	0.2832
0.2692	0.7320	0.2526	0.2681	0.2680
0.7570	0.7153	0.2432	0.7579	0.2847
0.7475	0.7329	0.7319	0.2675	0.2672
0.4880	0.5124	0.5124	0.4875	0.4876
0.2849	0.2428	0.2431	0.2844	0.7568
0.2837	0.2440	0.7150	0.7561	0.7563

Table 29: A 16-run IMSPE-optimal design in $[0,1]^5$ for prior $\mathrm{I}_{.75}$. This design was constructed using $N_{\text{des}} = 320 = 4 \times n \times d$ designs (particles) and $N_{\text{its}} = 640 = 2 \times N_{\text{des}}$ iterations for PSO. The IMSPE* value of this design is 0.1038.

x_1	x_2	x_3	x_4	x_5
0.5055	0.4920	0.4952	0.4926	0.4964
0.2581	0.2520	0.7499	0.7407	0.2541
0.7016	0.7677	0.2550	0.2952	0.2553
0.2582	0.7392	0.7520	0.2534	0.2534
0.6882	0.7734	0.7515	0.3111	0.7520
0.2592	0.7405	0.2554	0.2522	0.7510
0.2355	0.2970	0.2545	0.2968	0.2543
0.7416	0.2578	0.2794	0.2584	0.7396
0.2257	0.3075	0.7503	0.3114	0.7510
0.2296	0.7709	0.4681	0.7720	0.4669
0.7469	0.7406	0.2526	0.7418	0.7509
0.7038	0.2954	0.2556	0.7660	0.2540
0.7423	0.2577	0.7390	0.2581	0.2778
0.7490	0.7396	0.7508	0.7409	0.2518
0.6903	0.3114	0.7505	0.7738	0.7507
0.2591	0.2536	0.2533	0.7401	0.7510

Table 30: A 16-run W-IMSPE-optimal design in $[0,1]^5$ for prior W_W^{25}. This design was constructed using $N_{\text{des}} = 320 = 4 \times n \times d$ designs (particles) and $N_{\text{its}} = 640 = 2 \times N_{\text{des}}$ iterations for PSO. The first 90% of the iterations were based on 2^{11} Sobol´ draws, and the final iterations were based on 2^{17} Sobol´ draws. The W-IMSPE value of this design is 0.9352.

x_1	x_2	x_3	x_4	x_5
0.7183	0.7173	0.7495	0.7497	0.7497
0.5050	0.5047	0.4951	0.4954	0.4950
0.7350	0.2588	0.2646	0.2646	0.2649
0.2501	0.7164	0.7504	0.7502	0.2836
0.2501	0.2504	0.2829	0.7497	0.2821
0.2587	0.7357	0.2652	0.2651	0.2644
0.2502	0.2506	0.7497	0.2823	0.2816
0.7352	0.7353	0.7412	0.2647	0.2649
0.2491	0.2509	0.2825	0.2824	0.7495
0.7184	0.2505	0.7495	0.7492	0.2821
0.2502	0.7183	0.7498	0.2828	0.7498
0.7168	0.2501	0.7495	0.2822	0.7500
0.7350	0.7348	0.2644	0.2646	0.7415
0.7354	0.7353	0.2649	0.7412	0.2646
0.7172	0.2503	0.2820	0.7495	0.7496
0.2504	0.7184	0.2820	0.7498	0.7494

Table 31: A 16-run W-IMSPE-optimal design in $[0,1]^5$ for prior W_N^{25}. This design was constructed using $N_{\text{des}} = 320 = 4 \times n \times d$ designs (particles) and $N_{\text{its}} = 640 = 2 \times N_{\text{des}}$ iterations for PSO. The first 90% of the iterations were based on 2^{11} Sobol´ draws, and the final iterations were based on 2^{17} Sobol´ draws. The W-IMSPE value of this design is 4.4717.

x_1	x_2	x_3	x_4	x_5
0.7159	0.7158	0.7468	0.7468	0.7468
0.5063	0.5064	0.4937	0.4937	0.4936
0.7325	0.2614	0.2675	0.2674	0.2676
0.2532	0.7156	0.7469	0.7468	0.2844
0.2532	0.2530	0.2845	0.7469	0.2844
0.2613	0.7324	0.2675	0.2677	0.2676
0.2533	0.2532	0.7468	0.2840	0.2841
0.7324	0.7326	0.7386	0.2675	0.2675
0.2532	0.2532	0.2843	0.2843	0.7468
0.7160	0.2533	0.7467	0.7467	0.2840
0.2533	0.7159	0.7468	0.2840	0.7467
0.7160	0.2533	0.7467	0.2840	0.7466
0.7324	0.7324	0.2675	0.2675	0.7386
0.7324	0.7325	0.2676	0.7388	0.2676
0.7157	0.2532	0.2843	0.7468	0.7468
0.2531	0.7156	0.2845	0.7469	0.7470

Table 32: A 16-run W-IMSPE-optimal design in $[0,1]^5$ for prior W_N^5. This design was constructed using $N_{\text{des}} = 320 = 4 \times n \times d$ designs (particles) and $N_{\text{its}} = 640 = 2 \times N_{\text{des}}$ iterations for PSO. The first 90% of the iterations were based on 2^{11} Sobol´ draws, and the final iterations were based on 2^{17} Sobol´ draws. The W-IMSPE value of this design is 2.2396.

x_1	x_2	x_3	x_4	x_5
0.7167	0.7168	0.7576	0.7578	0.7575
0.5115	0.5115	0.4885	0.4885	0.4885
0.7339	0.2524	0.2661	0.2660	0.2662
0.2421	0.7160	0.7577	0.7579	0.2838
0.2424	0.2422	0.2831	0.7578	0.2838
0.2522	0.7336	0.2663	0.2662	0.2662
0.2423	0.2421	0.7576	0.2836	0.2836
0.7334	0.7337	0.7479	0.2662	0.2662
0.2427	0.2425	0.2829	0.2831	0.7579
0.7171	0.2425	0.7574	0.7576	0.2828
0.2422	0.7165	0.7576	0.2834	0.7578
0.7166	0.2423	0.7579	0.2837	0.7577
0.7341	0.7339	0.2664	0.2659	0.7476
0.7337	0.7340	0.2662	0.7475	0.2659
0.7173	0.2427	0.2829	0.7576	0.7575
0.2426	0.7170	0.2828	0.7575	0.7578

Table 33: A 16-run W-IMSPE-optimal design in $[0,1]^5$ for prior W^U. This design was constructed using $N_{\text{des}} = 320 = 4 \times n \times d$ designs (particles) and $N_{\text{its}} = 640 = 2 \times N_{\text{des}}$ iterations for PSO. The first 90% of the iterations were based on 2^{11} Sobol´ draws, and the final iterations were based on 2^{17} Sobol´ draws. The W-IMSPE value of this design is 0.4580.

x_1	x_2	x_3	x_4	x_5
0.3422	0.7876	0.8260	0.7925	0.1737
0.6367	0.2539	0.7422	0.8179	0.8376
0.8243	0.8339	0.7720	0.4996	0.5142
0.7476	0.1956	0.7842	0.1918	0.2159
0.4103	0.3286	0.3671	0.4739	0.1484
0.8023	0.1751	0.1811	0.5489	0.5358
0.8111	0.5590	0.4521	0.1766	0.8159
0.8295	0.5041	0.4777	0.8280	0.2246
0.1658	0.1457	0.7007	0.6668	0.4242
0.6174	0.8149	0.1631	0.2525	0.2399
0.1640	0.6638	0.5880	0.1474	0.3224
0.5946	0.7784	0.2325	0.7786	0.7587
0.4215	0.4747	0.8545	0.3355	0.6512
0.1913	0.8170	0.5428	0.5152	0.8360
0.2602	0.2083	0.2240	0.2078	0.7781
0.1897	0.5050	0.1664	0.8190	0.4516

Table 34: A 16-run IMSPE-optimal design in $[0,1]^5$ for prior I_M. This design was constructed using $N_{\mathrm{des}} = 320 = 4 \times n \times d$ designs (particles) and $N_{\mathrm{its}} = 640 = 2 \times N_{\mathrm{des}}$ iterations for PSO. The IMSPE* value of this design is 0.4259.

x_1	x_2	x_3	x_4	x_5
0.5041	0.4243	0.1861	0.1857	0.1858
0.4913	0.6760	0.5004	0.1426	0.4999
0.7783	0.2954	0.5008	0.5009	0.5000
0.4911	0.6752	0.4994	0.5008	0.8576
0.5039	0.4245	0.8141	0.1859	0.8139
0.4905	0.6769	0.1435	0.4997	0.4997
0.4908	0.6746	0.4999	0.8574	0.5005
0.2456	0.2688	0.4990	0.5003	0.4999
0.5041	0.4247	0.8142	0.8142	0.1864
0.5041	0.4245	0.1857	0.1862	0.8142
0.4904	0.6762	0.5003	0.5001	0.1432
0.5037	0.4241	0.1853	0.8142	0.8136
0.5040	0.4245	0.1860	0.8138	0.1855
0.5041	0.4247	0.8142	0.8140	0.8142
0.4851	0.6766	0.8564	0.5002	0.5000
0.5039	0.4247	0.8144	0.1860	0.1858

B Empirical MSPE Tables

Table 35: The 75$^{\text{th}}$ percentile of the 40 EMSPE values for the 10 designs and the 7 test-beds studied when $(n, d) = (10, 2)$.

Design		$y_{\text{test}}(\cdot)$ Test-bed Correlation Setting						
		Deterministically Common			*Stochastically Common*			*Mixed Activity*
		$\text{T}_{.25}^{DC}$	$\text{T}_{.5}^{DC}$	$\text{T}_{.75}^{DC}$	$\text{T}_{.25}^{SC}$	$\text{T}_{.5}^{SC}$	$\text{T}_{.75}^{SC}$	T^{M}
IMSPE-optimal	$\text{I}_{.25}$	2.3962	0.5381	0.0861	2.1022	1.0055	0.0846	0.0951
	$\text{I}_{.5}$	2.3050	0.6251	0.0412	2.2177	0.6173	0.0549	0.1203
	$\text{I}_{.75}$	2.6371	0.6957	0.0431	1.9086	0.5479	0.0407	0.0724
	I_{M}	2.4852	0.6866	0.0443	2.1208	0.6276	0.0509	0.0650
Space-Filling	MmLHD	3.0648	1.0474	0.1214	2.8343	1.0456	0.1000	0.0929
	mARDLHD	2.9056	0.7807	0.0590	2.1682	0.6564	0.0704	0.1696
W-IMSPE-optimal	$\text{W}_{W}^{.25}$	2.0434	0.8036	0.0459	1.9281	0.5358	0.0390	0.0910
	$\text{W}_{N}^{.25}$	2.1269	0.5418	0.0786	2.1215	0.6901	0.0621	0.2219
	$\text{W}_{N}^{.5}$	1.9084	0.4887	0.0442	2.1094	0.6190	0.0588	0.1272
	W^{U}	2.1461	0.5707	0.0492	2.1289	0.6478	0.0518	0.1199

Table 36: The 75$^{\text{th}}$ percentile of the 40 EMSPE values for the 10 designs and the 7 test-beds studied when $(n, d) = (15, 3)$.

Design		$y_{\text{test}}(\cdot)$ Test-bed Correlation Setting						
		Deterministically Common			*Stochastically Common*			*Mixed Activity*
		$\text{T}_{.25}^{DC}$	$\text{T}_{.5}^{DC}$	$\text{T}_{.75}^{DC}$	$\text{T}_{.25}^{SC}$	$\text{T}_{.5}^{SC}$	$\text{T}_{.75}^{SC}$	T^{M}
IMSPE-optimal	$\text{I}_{.25}$	10.1672	10.1397	5.2803	12.4026	11.6966	6.0658	15.4568
	$\text{I}_{.5}$	9.6092	9.8692	5.2531	10.8580	11.3925	6.1101	13.8715
	$\text{I}_{.75}$	9.0840	9.3440	5.2540	11.6745	11.5631	6.1290	14.3699
	I_{M}	9.2493	9.9597	5.3649	11.1252	12.2797	6.0222	14.3430
Space-Filling	MmLHD	11.3772	9.7760	5.3131	12.3688	11.4299	5.7776	17.1289
	mARDLHD	10.3812	9.9489	5.6256	13.3217	12.5663	5.1735	14.7193
W-IMSPE-optimal	$\text{W}_{W}^{.25}$	9.0945	9.6982	5.1102	11.4046	10.9751	6.0931	14.6611
	$\text{W}_{N}^{.25}$	10.0184	10.3119	5.5750	12.1545	13.2955	5.9280	15.3386
	$\text{W}_{N}^{.5}$	9.6479	9.8574	5.2616	10.8857	11.3761	6.1153	13.9513
	W^{U}	10.4110	9.8446	5.8186	12.9295	14.1332	5.8886	15.1565

Table 37: The 75$^{\text{th}}$ percentile of the 40 EMSPE values for the 10 designs and the 7 test-beds studied when $(n, d) = (16, 5)$.

Design		$y_{\text{test}}(\cdot)$ Test-bed Correlation Setting						
		Deterministically Common			*Stochastically Common*			*Mixed Activity*
		$\text{T}_{.25}^{DC}$	$\text{T}_{.5}^{DC}$	$\text{T}_{.75}^{DC}$	$\text{T}_{.25}^{SC}$	$\text{T}_{.5}^{SC}$	$\text{T}_{.75}^{SC}$	T^{M}
IMSPE-optimal	$\text{I}_{.25}$	9.9936	8.8786	4.2444	9.1297	8.5275	5.6790	10.2960
	$\text{I}_{.5}$	10.1695	8.6785	4.8758	10.1265	9.8518	5.9282	12.1609
	$\text{I}_{.75}$	9.6072	9.2665	4.1770	10.0072	9.8715	5.8765	10.6089
	I_{M}	10.6767	10.7250	4.3979	10.9395	10.0888	7.2397	11.1006
Space-Filling	MmLHD	12.8333	9.9305	5.3857	12.8132	11.2207	5.8510	13.1504
	mARDLHD	13.7438	11.8078	4.4500	13.7231	11.1600	5.8705	13.2309
W-IMSPE-optimal	$\text{W}_{W}^{.25}$	9.8386	9.2206	4.3338	9.7061	9.8746	6.4234	11.9875
	$\text{W}_{N}^{.25}$	10.0710	9.2415	4.3940	9.6548	9.3707	6.2171	11.1714
	$\text{W}_{N}^{.5}$	9.6378	9.0647	4.4087	9.4531	9.3876	5.4871	12.0629
	W^{U}	12.8968	10.4735	5.1856	14.5866	11.0020	5.9825	13.2036

C Design Construction Times

The IMSPE- and W-IMSPE-optimal designs used in the simulation study of Section 6 were constructed on various compute machines. Computation times for each of the designs having $(n, d) \in \{(10, 2), (15, 3), (30, 3)\}$ are listed in Tables 38–40, respectively. For the set of 16×5 designs, Designs $\text{I}_{.25}$, $\text{I}_{.5}$, $\text{I}_{.75}$ and I_{M} (all IMSPE-optimal designs) were computed using a Dual Quad Core Xeon E5430 with 2.66 GHz processor speed and 32GB RAM, and took an average of 491.9 seconds to compute. The time needed to compute the W-IMSPE-optimal designs was not recorded.

Table 38: Computation details for the set of 10×2 designs. The average construction time in seconds is given for designs of the same type that used similar machines.

design label	time (s)	compute machine (# cores used for MATLAB worker pool)
$\text{I}_{.25}$, $\text{I}_{.5}$, $\text{I}_{.75}$, I_{M}	22	2x Quad Core Xeon E5430, 2.66 GHz, 32 GB
$\text{W}_{N}^{.25}$, $\text{W}_{N}^{.5}$, $\text{W}_{W}^{.25}$*	7,217	4x Eight Core Xeon E7-4830, 2.13GHz, 128 GB (12) *or* 694 Node Xeon X5650, 2.67GHz, 48 GB/node (12, one node)
W^{U}	7,861	2x Quad Core Xeon E5430, 2.66 GHz, 32 GB (3)

*Design $\text{W}_{W}^{.25}$ took a similar time to $\text{W}_{N}^{.25}$ and $\text{W}_{N}^{.5}$, but the precise time was not recorded.

Table 39: Computation details for the set of 15×3 designs. The average construction time in seconds is given for designs of the same type that used similar machines.

design label	time (s)	compute machine (# cores used for MATLAB worker pool)
$I_{.25}$, $I_{.5}$, $I_{.75}$, I_M	116	2x Quad Core Xeon E5430, 2.66 GHz, 32 GB
$W_W^{.25}$ and $W_N^{.25}$	185,986	2x Eight Core Xeon E5-2680, 2.7 GHz, 384 GB (3)
$W_N^{.5}$	203,566	2x Quad Core Xeon E5430, 2.66 GHz, 32 GB (3)
W^U	209,442	2x Six Core Xeon X5650, 2.66 GHz, 48 GB (3)

Table 40: Computation details for the set of 30×3 designs. The average construction time in seconds is given for designs of the same type that used similar machines.

design label	time (s)	compute machine (# cores used for MATLAB worker pool)
$I_{.25}$, $I_{.5}$, $I_{.75}$, I_M	848.4	2x Quad Core Xeon E5430, 2.66 GHz, 32 GB
$W_W^{.25}$	1,861,417	2x Quad Core Xeon E5430, 2.66 GHz, 32 GB (3)
$W_N^{.25}$ and $W_N^{.5}$	1,326,097	2x Eight Core Xeon E5-2680, 2.7 GHz, 384 GB (3)

D Space-filling Designs

The space-filling designs used in Section 6 were obtained from a website (van Dam et al. 2013) and are given in this appendix.

Table 41: The 10-run MmLHD in $[0,1]^2$ obtained from a website containing space-filling designs (van Dam et al. 2013).

x_1	x_2
0.0000	0.2222
0.1111	0.5556
0.2222	0.8889
0.3333	0.1111
0.4444	0.4444
0.5556	0.7778
0.6667	0.0000
0.7778	0.3333
0.8889	0.6667
1.0000	1.0000

Table 42: The 10-run mARDLHD in $[0,1]^2$ obtained from a website containing space-filling designs (van Dam et al. 2013).

x_1	x_2
0.0000	0.3333
0.1111	0.7778
0.2222	0.0000
0.3333	0.4444
0.4444	0.8889
0.5556	0.1111
0.6667	0.5556
0.7778	1.0000
0.8889	0.2222
1.0000	0.6667

Table 43: The 15-run MmLHD in $[0,1]^3$ obtained from a website containing space-filling designs (van Dam et al. 2013).

x_1	x_2	x_3
0.0000	0.3571	0.4286
0.0714	0.8571	0.2857
0.1429	0.2857	0.9286
0.2143	0.7857	0.7857
0.2857	0.0714	0.1429
0.3571	0.5714	0.0000
0.4286	0.0000	0.6429
0.5000	0.5000	0.5000
0.5714	1.0000	0.3571
0.6429	0.4286	1.0000
0.7143	0.9286	0.8571
0.7857	0.2143	0.2143
0.8571	0.7143	0.0714
0.9286	0.1429	0.7143
1.0000	0.6429	0.5714

Table 44: The 15-run mARDLHD in $[0,1]^3$ obtained from a website containing space-filling designs (van Dam et al. 2013).

x_1	x_2	x_3
0.0000	0.3571	0.5714
0.0714	0.8571	0.7143
0.1429	0.7857	0.2143
0.2143	0.2857	0.0714
0.2857	0.2143	0.9286
0.3571	0.0000	0.4286
0.4286	0.7143	1.0000
0.5000	0.5000	0.5000
0.5714	0.9286	0.1429
0.6429	1.0000	0.6429
0.7143	0.4286	0.0000
0.7857	0.1429	0.7857
0.8571	0.0714	0.2857
0.9286	0.5714	0.8571
1.0000	0.6429	0.3571

Table 45: The 30-run MmLHD in $[0,1]^3$ obtained from a website containing space-filling designs (van Dam et al. 2013).

x_1	x_2	x_3
0.0000	0.1724	0.5172
0.0345	0.4483	0.1724
0.0690	0.6207	0.7586
0.1034	0.7586	0.4138
0.1379	0.8966	0.0690
0.1724	0.0690	0.2069
0.2069	0.2759	0.8276
0.2414	0.9655	0.7241
0.2759	0.4138	0.4483
0.3103	0.0000	0.6207
0.3448	0.3103	0.0000
0.3793	0.6897	0.9310
0.4138	0.6552	0.1379
0.4483	0.7241	0.5517
0.4828	1.0000	0.3103
0.5172	0.1379	0.9655
0.5517	0.3793	0.6897
0.5862	0.1034	0.2414
0.6207	0.9310	0.7931
0.6552	0.4828	0.3448
0.6897	0.0345	0.5862
0.7241	0.5517	1.0000
0.7586	0.7931	0.1034
0.7931	0.3448	0.0345
0.8276	0.8621	0.4828
0.8621	0.2069	0.8621
0.8966	0.5172	0.6552
0.9310	0.2414	0.3793
0.9655	0.8276	0.8966
1.0000	0.5862	0.2759

Table 46: The 30-run mARDLHD in $[0,1]^3$ obtained from a website containing space-filling designs (van Dam et al. 2013).

x_1	x_2	x_3
0.0000	0.3103	0.6897
0.0345	0.6552	0.4483
0.0690	0.2069	0.2414
0.1034	0.6897	0.8276
0.1379	0.5517	0.1034
0.1724	0.8966	0.2069
0.2069	0.9655	0.6207
0.2414	0.0690	0.7241
0.2759	0.3793	0.9655
0.3103	0.3448	0.4828
0.3448	0.0000	0.3448
0.3793	0.2759	0.0345
0.4138	0.7931	0.9310
0.4483	0.7241	0.0000
0.4828	0.7586	0.5862
0.5172	1.0000	0.3103
0.5517	0.1379	0.8966
0.5862	0.5172	0.2759
0.6207	0.4483	0.6552
0.6552	0.0345	0.5517
0.6897	0.1034	0.1724
0.7241	0.4828	1.0000
0.7586	0.8621	0.8621
0.7931	0.8276	0.1379
0.8276	0.9310	0.5172
0.8621	0.4138	0.0690
0.8966	0.1724	0.7931
0.9310	0.2414	0.4138
0.9655	0.6207	0.3793
1.0000	0.5862	0.7586

Table 47: The 16-run MmLHD in $[0,1]^5$ obtained from a website containing space-filling designs (van Dam et al. 2013).

x_1	x_2	x_3	x_4	x_5
0.0000	0.5333	0.5333	0.2000	0.1333
0.0667	0.3333	0.6000	1.0000	0.4000
0.1333	0.2667	0.6667	0.3333	0.9333
0.2000	1.0000	0.7333	0.6000	0.6667
0.2667	0.0667	0.0000	0.4667	0.4667
0.3333	0.8667	0.0667	0.7333	0.2000
0.4000	0.8000	0.1333	0.0667	0.7333
0.4667	0.6000	0.2000	0.8667	1.0000
0.5333	0.0000	0.8667	0.4000	0.2667
0.6000	0.6667	0.9333	0.0000	0.5333
0.6667	0.7333	0.8000	0.6667	0.0000
0.7333	0.4667	1.0000	0.8000	0.8000
0.8000	0.4000	0.2667	0.1333	0.0667
0.8667	0.2000	0.3333	0.9333	0.3333
0.9333	0.1333	0.4667	0.2667	0.8667
1.0000	0.9333	0.4000	0.5333	0.6000

Table 48: The 16-run mARDLHD in $[0,1]^5$ obtained from a website containing space-filling designs (van Dam et al. 2013).

x_1	x_2	x_3	x_4	x_5
0.0000	0.6667	0.6000	0.8000	0.2000
0.0667	0.5333	0.3333	0.0000	0.3333
0.1333	0.0667	0.2000	0.6667	0.6000
0.2000	0.1333	1.0000	0.4000	0.4667
0.2667	0.8667	0.0667	0.5333	0.8667
0.3333	0.9333	0.8667	0.3333	0.8000
0.4000	0.4667	0.7333	1.0000	0.9333
0.4667	0.2667	0.4667	0.1333	1.0000
0.5333	0.6000	0.0000	0.6000	0.0667
0.6000	0.7333	0.8000	0.2667	0.0000
0.6667	0.2000	0.6667	0.9333	0.1333
0.7333	0.0000	0.4000	0.2000	0.2667
0.8000	1.0000	0.5333	0.8667	0.4000
0.8667	0.8000	0.2667	0.0667	0.5333
0.9333	0.3333	0.1333	0.7333	0.7333
1.0000	0.4000	0.9333	0.4667	0.6667